IEEE Access
Multidisciplinary ⋮ Rapid Review ⋮ Open Access Journal

Received 1 March 2023, accepted 17 March 2023, date of publication 31 March 2023, date of current version 2 May 2023.

Digital Object Identifier 10.1109/ACCESS.2023.3263490

RESEARCH ARTICLE

A Comparative Study Between Bayesian Network and Hybrid Statistical Predictive Models for Proactive Power System Network Resilience Enhancement Operational Planning

SAMUEL O. OMOGOYE, (Member, IEEE), KOMLA A. FOLLY, (Senior Member, IEEE), AND KEHINDE O. AWODELE, (Member, IEEE)

Department of Electrical Engineering, University of Cape Town, Cape Town 7701, South Africa

Corresponding author: Samuel O. Omogoye (samelect2017@gmail.com)

This work was supported by University of Cape Town, South Africa, Tertiary Education Trust Fund-PhD Grant(2019-2021), Nigeria, and in part by the National Research Foundation- South Africa, grant number 118550.

ABSTRACT Enhancing the operational resilience of the distribution system network (DSN) proactively in a hurricane-prone region requires a pre-hurricane event DSN optimization model, built on accurate hurricane-induced DSN line damage prediction scenarios. In the past, the resilience evaluation methods such as statistical sequential and non-sequential Monte Carlo simulation (MCS) contingency-based technique, and Machine learning-based Bayesian Networks (BN) technique, have been proposed to strengthen the operational resilience of the DSN proactively against forecasted oncoming hurricane events. However, a comparative study is largely unexplored to evaluate which of these two methods is best for proactive operational planning decision-making against forecasted oncoming hurricane events. In this paper, the Bayesian network (BN) and hybrid statistical DSN's Fragility-curve (FC)-Monte Carlo simulation (MCS)-Scenario reduction (SCENRED) predictive algorithms were developed. The DSN line fault prediction scenarios simulated leveraging the predicted oncoming hurricane Ewiniar data were utilized to perform pre-hurricane DSN optimization to proactively decrease the DSN expected load loss. The pre-event system optimization problems were formulated in a mixed integer linear programming (MILP) approach and solved using a CPLEX solver in the general algebraic modelling system (GAMS) on a redesigned 48-bus DSN. The simulated initial expected load loss of 39% of 35 MW was decreased to 35.34%, and then to 30.71% with the use of hybrid statistical DSN's FC-MCS-SCENRED, and the BN-DSN predictive models. These results were validated using the Electrical transient analyzer program (ETAP). This study confirmed that the BN-DSN predictive model is a better operational planning tool compared to hybrid statistical DSN's line FC-MCS-SCENRED predictive model.

INDEX TERMS Bayesian network (BN) predictive algorithm, distribution system network (DSN), hurricane events, hybrid statistical DSN's line FC-MCS-SCENRED predictive algorithm, pre-hurricane event's optimal DSN reconfiguration and resource allocation.

NOMENCLATURE

A. SETS INDICES

x, y	Indices for grid buses
a, b	Indices for lines
ψ_x	Set of bus bar joined to bus x
l	Line index
t	Time index
PSN	Power system network
HS	Hurricane event wind speed data

The associate editor coordinating the review of this manuscript and approving it for publication was Yiqi Liu.

B. PARAMETERS

$P^{D}_{t,x}$ $Q^{D}_{t,x}$	Real and reactive power expected at bus- bar "x", time "t"
L_{cap}	Line capacity
E_F	Events forecast time
S^{RCS}_{Wa}	Consider that point "a" has a remote-controlled switch, then the binary parameter is equal to 1
M	A suitably large positive number
$R_l X_l$	Resistance, Reactance of the line
$P^{e_o}_{pre}$, P^{lds}_{pre}	pre-hurricane event DSN active load.
$S_{ST}(a)$	Total time required to change switch status at point "a"
RCS"t"	Remote-controlled switching time.
ω^{F}_{x}	Weight factor at load bus "x".
L^{DS}	The binary parameter will be 0, at a damaged scenario (s) of the line"l".
$V_{max,} V_{min}$	Maximum and minimum operational constrained. Voltage(s),
S_{max}	Grid maximum apparent power.
$P^{DG}_{x,max}$, $P^{DG}_{x,min}$	The maximum and minimum real power output of the DGs at bus "x".
$Q^{DG}_{x,max}$, $Q^{DG}_{x,min}$	The maximum and minimum reactive power output of the DGs at bus "x".
$P^{PV}_{t,x(max)}$	The maximum PV active power output at bus "x", time, "t"
$SL_{lol1}(I)$, $SL_{lol2}(I)$, $SL_{lol3}(I)$	Value of load loss at the bus "x", in $/MWh

C. VARIABLES

OF	Objective function
$P^{AC_{flow}}_{t,l}$, $Q^{AC_{flow}}_{t,l}$	Real and reactive AC power flow in the line at a time "t".
$P^{LS}_{t',x}$, $Q^{LS}_{t',x}$	Real and reactive load-shedding at bus "x", time "t'".
$P^{DG}_{out@t,x}$, $Q^{DG}_{out@t,x}$	DG's Real and reactive output power at bus "x", time, "t".
$P^{PV}_{out@t,x}$, $Q^{PV}_{out@t,x}$	Photovoltaic Real and reactive output power at bus "x", time "t"
$P^{WT}_{out@t,x}$, $Q^{WT}_{out@t,x}$	Wind turbine (WT) real and reactive output power at bus "x" time, "t".
$S_{w(t,l)}$	The-binary variable = 1, for a closed switch on line set "l," otherwise = 0 at a time "t".
$\acute{R}_{t',l}$	For a repairable line "l" status at time "t", The binary variable = 1. Otherwise, 0.
$\varsigma_{sw(t,l)}$	Consider that the switch status changes for line "l" at a time "t", the binary variable = 1
$\delta_{t,x}$	If the DG at bus-bar "x", at a time "t" is planned then the binary variable = 1, otherwise = 0.
$V_{t,x}$	The magnitude of the voltage at bus "x", time, "t".
$V_{t,y}$	The magnitude of the voltage at bus "y", time, "t".
$\gamma_{x,y,t}$	If bus "y" is the parent of bus "x", at a time "t", binary variable = 1.
$P^{LS}_{t,x}$	Interrupted real power at bus "x", in MW

I. INTRODUCTION

A reliable electricity supply supports human existence, societal growth, and civilization globally. Regrettably, power system network (PSN) infrastructures are usually subjected to damage during high impact low likelihood (HILL) events. The HILL events could either be extreme weather events that are predictable and unpredictable or human-induced power system operational errors. These two major sources of fault usually result in cascaded power outages with a lot of loss of revenue. From the published literature, the study of the causes of the widespread power blackout conducted in the United States of America (U.S.A) in 2008, showed that between 1984 and the year 2006, 933 events resulted in large-scale power outages. 44% of these events were caused by natural events such as hurricane events [1], [2]. The United States Department of Energy (US-DOE) data showed that out of 1,333 power system network damages recorded between 1992 and the year 2011, almost 78% were caused by extreme weather events [3]. Hurricane event-induced power outages on the DSN are very common around the globe these days due to global warming [4]. For example, on the 11th of June 2018, hurricane Ewiniar dumped very heavy rainfall in Vietnam along the western coast of the South China sea. In this event, fourteen (14) people died. Loss of social infrastructures worth ¥5.19 billion ($749 million) was recorded [5], [6]. Over the past 50 years, it has been documented that more than 30 tropical cyclones have affected the South African mainland [7]. On the 29th of August 2021, a catastrophic category-4 Hurricane Ida hit Louisiana tearing off the basic infrastructures like hospital roofs, the DSN, etc. In this incident, millions of people were thrown into a total power blackout. Over 1 million electricity end-users experienced a total blackout in New Orleans, Louisiana and Mississippi, with a record of two (2) lives lost in Louisiana [8]. In a report presented on CNN

by Rachel Ramirez, it was noted that researchers raised alarm on increased large-scale power outages due to the extreme weather around Texas, Michigan and California. About 1,500 large-scale power outages were recorded from the year 2000 to 2022 [9]. The July 8th 2022 flood event in Nigeria threw several people living around Lekki, Ikoyi, and Victoria Island of Lagos State into a total blackout for several days due to the power system sub-station and power equipment that was submerged by the flood [10]. The Africa report states that ''there is hardly any work done on improving the institution that works on disaster management in Nigeria'' [11]. This was evident as the report of 29th October 2022, indicated that twenty-seven (27) out of thirty-six (36) states in Nigeria have been hit by the flood. In this event, six hundred and three (603) people died. Two million-five hundred and four thousand, and ninety-five (2,504,095) people were affected. Two thousand four hundred and seven (2,407) people were injured, while one-million, three hundred and two thousand, five hundred and eighty-nine (1,302,589) people were displaced [11]. In view of this, this article is motivated to focus on improving the operational resilience of the DSN against predictable extreme weather events like hurricanes. The goal is to lessen the expected load loss, and the impact of the protracted widespread power outages proactively, leveraging the proposed DSN predictive algorithms in this paper for the DSN proactive operational planning decision-making.

A comprehensive literature review of the steps and strategies utilized to achieve power system resilience improvement against HILL events such as hurricanes was presented in [12] and [13]. These papers suggested the need to change the reactive operational resilience improvement techniques proposed by many researchers in assessing the resilience improvement of the DSN against hurricane events, to a more defensive proactive operational resilience improvement approach [14]. In Omogoye et al., [15], [16], it was revealed that the prospective statistical regression methods (such as the generalized linear model (GLM), generalized additive model (GAM), system tree-approach mining models (STMM),) and the power system topology (PST)-based resilience evaluation approach (such as the predictive DSN line's FC-MCS) have been utilized to assess hurricane-caused DSN line faults in the past. The GLM, GAM, and STMM approaches are grouped as system-level damage predictive algorithms [17]. These approaches are appropriate for long-term PSN infrastructural planning. However, an increase in PSN line fault prediction approximation error limits their application for the short-term operational resilience improvement planning against predicted oncoming hurricane events. Similarly, the power system topology (PST)-based resilience evaluation approach which includes a combination of a statistical DSN line's FC-MCS predictive model is also known to introduce high computational complexity due to the use of 1000 or more predicted system line fault scenarios for a proactive stochastic system optimization problem formulation and simulation as demonstrated in [15], [16], and [18]. It is worth noting that in all the prospective methods aforementioned above, the uncertain nature of the hurricane event on the PSN was not captured. Therefore, to address the problem of neglect of the non-stationary nature of hurricane events on the PSN when modelling the DSN line fault predictive algorithm, a machine learning dynamic BN-DSN line fault predictive algorithm was proposed in [19]. The proposed BN-DSN predictive model considered fully the uncertainties of the hurricane events on the modified IEEE 14-bus DSN lines, to predict the DSN line faults. However, the BN-DSN line prediction validation model was not developed in [19]. The improved hybrid statistical DSN line's FC-MCS-SCENRED predictive algorithm that validates the proposed BN-DSN predictive model in [19] was presented in [20]. The study where both the proposed BN-DSN and hybrid statistical DSN line's FC-MCS-SCENRED predictive algorithms were developed using IEEE 15-bus to determine their prediction accuracy can be found in [21]. The study presented the full analysis of the two predictive algorithms' accuracy and concluded that the proposed BN-DSN predictive model outperformed the combined statistical DSN's line FC-MCS-SCENRED model. However, the proposed model in [21] was never tested with a proactive system optimization model for impact assessment as regards the reduction in the expected load loss. Other literature such as [16], [19], and [22] also supported the proposed BN-DSN predictive model as a better operational planning decision-making tool for the distribution system operators (DSO) compared to the combined statistical DSN's line FC-MCS-SCENRED predictive algorithm. Generally, studies to corroborate or support this claim are largely unexplored and hence, presents a research gap.

To contribute to knowledge from this perspective, this study presents a comparative performance-based analysis between the proposed BN-DSN and combined statistical DSN lines FC-MCS-SCENRED predictive algorithms, to determine the best DSN predictive algorithm that can reduce the expected load loss proactively from unstoppable forecasted oncoming hurricane events. This type of system operation planning tool would enhance the best proactive operational planning decision-making by the DSO to strengthen the DSN operational resilience planning against the forecasted oncoming hurricane event in the future. It will also help the DSO to assess the power system network risk and vulnerability against any future predictable extreme weather events since the extreme weather events will not stop and cannot be controlled.

The novelties introduced in the study, include the development of different predictable weather-dependent DSN line fault predictive algorithms, conducting performance-based tests on them for proactive operational resilience enhancement against hurricane events, and integrating the best predictive algorithm in a proactive system optimization model to decrease the expected load loss. The objectives are to: reduce the revenue deficit for the power utility companies; and reduce the protracted power outages of electricity end-users

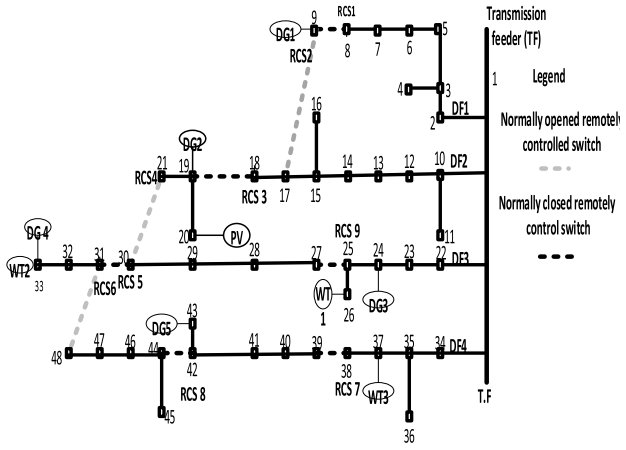

FIGURE 1. Redesigned 48-bus DSN one-line diagram [18], [24].

to enhance electricity end-users' survivability after a hurricane event in the future. Hence, the operational resilience of the DSN lines against predictable extreme weather events like a hurricane is enhanced. This goal motivates this study.

The remaining sections of this paper are arranged as follows: Section II presents research data and the methodologies. In section III, the comparative analysis of the efficiency of the two proposed system line fault predictive algorithms is presented. Section IV discusses the pre-hurricane event DSN reconfiguration and resource planning for the system's operational resilience improvement. Section V gives detailed information on the system optimization simulation results analysis, while section VI, concludes the paper.

II. RESEARCH DATA AND METHODS

A. DESCRIPTION OF RESEARCH DATA, MODIFIED 48-BUS DSN, AND SOFTWARE TOOLS

Hurricane event is the natural disaster considered in this article. This is due to its harsh impact on the DSN [23]. The past hurricane events' wind speed intensity measured in meters per second (m/s) called "typhoon_data_mat" that was collected between 1949 to 2019 from Shenzhen region in China was utilised to train the prospective combined statistical DSN line's FC-MCS-SCENRED and the BN-DSN line fault predictive algorithms in this study. The predicted oncoming hurricane Ewiniar data in [19], was utilized to perform the DSN line fault prediction. The small size of the redesigned 48-bus DSN was selected for this research investigation because of the experienced complexity associated with the BN-DSN design calculation using a larger network. Fig.1 shows a region-bound one-line diagram of the redesigned 48-bus DSN with a voltage capacity of 200 kV, one (1) transmission bus bar, four (4) distribution feeders (DF1, DF2, DF3, and DF4) with an approximate thermal capacity of 10 MVA, three (3) assumed normally open remote-controlled switches located on buses 9, 21, and 31, and six (6) assumed normally closed remote-controlled switches located on buses

TABLE 1. The redesigned 48-bus system's load demand profile [18], [24].

Time (Hour)	Daily actual load demand (p.u)	Percentage of daily load demand (%)
0-1	1.8900	54
1-2	1.8200	52
2-3	1.7500	50
3-4	1.4000	40
4-5	1.4000	40
5-6	1.0500	30
6-7	1.2250	35
7-8	1.5750	45
8-9	1.7500	50
9-10	2.3100	66
10-11	2.5900	74
11-12	2.5900	74
12-13	2.5200	72
13-14	2.6250	75
14-15	2.7300	78
15-16	2.6950	77
16-17	2.3800	68
17-18	2.5200	72
18-19	3.1500	90
19-20	3.5000	100
20-21	3.5000	100
21-22	3.5000	100
22-23	3.0800	88
23-24	2.5000	71

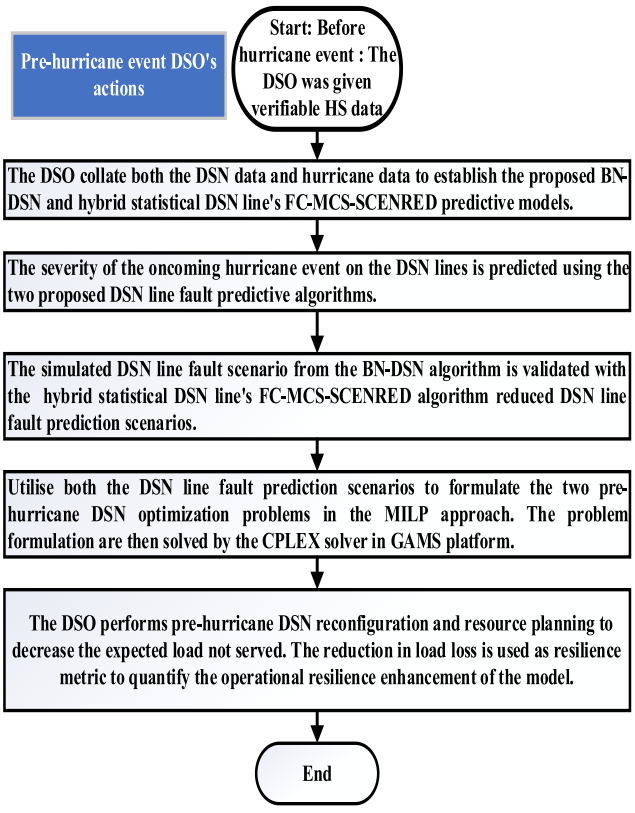

FIGURE 2. The proposed pre-hurricane events DSN optimization method.

8, 18, 25, 30, 38, and 42 respectively. It also has three (3) wind turbines (WTs) located on buses 26, 33, and 37, five dispatchable distributed generators (DGs) situated on buses 9, 19, 24, 33, 43, and a single photovoltaic (PV) panel installed

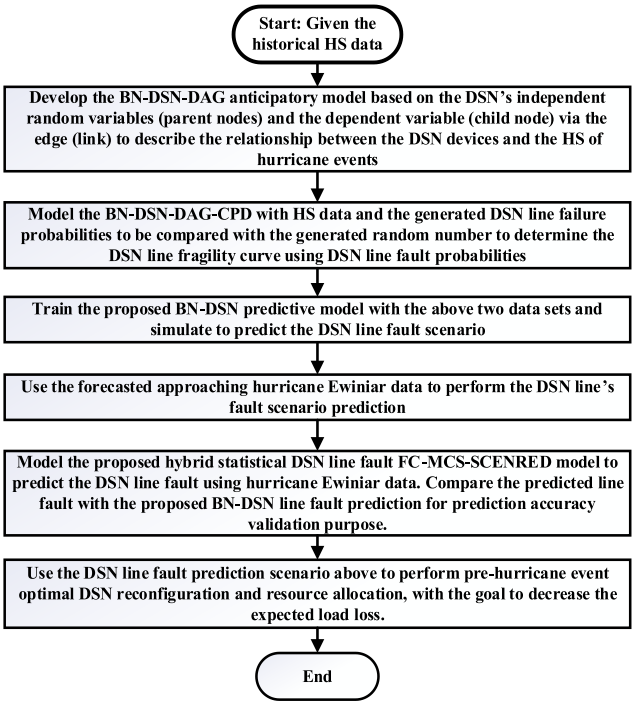

FIGURE 3. The proposed BN-DSN line fault model flow chart [21].

on bus 20 [24]. The system MVA base is 10 MVA and the minimum and maximum levels of voltage magnitude at the DSN bus are 0.95 and 1.05 p. u, respectively [24]. Table 1 presents the redesigned 48-bus DSN's daily load demand profile. The distributed energy resources (DER) unit locations and their ratings, the daily PV and WTs power output data can be found in [24]. The DSN is assumed to have nine (9) remote-controlled switches (RCSs) located on buses 8, 9, 18, 21, 25, 30, 31, 38, and 42. Software tools which include Microsoft-word package, Excel spreadsheet, Mendeley reference manager, R-software, GAMS, and ETAP were employed for this research investigation. A personal computer with an Intel core i3-6100UCPU@2.30 GHz processor with 8 GB RAM was utilized to perform all simulations.

B. RESEARCH METHODOLOGIES

The prospective procedural steps to perform the pre-hurricane DSN optimization to minimize the expected load loss using the DSN line faults prediction scenarios from the two prospective hurricane-induced DSN line fault predictive algorithms are presented in Fig. 2.

1) MODELLING OF THE PROBABILISTIC PREDICTIVE BN-DSN MODEL BASED ON THE PREDICTED ONCOMING HURRICANE EVENT

Figure 3 shows the overview of the proposed BN-DSN predictive algorithm flow chart. The detailed step-by-step design procedures for the proposed BN-DSN predictive model can be found in [21]. The prediction accuracy analysis is the focus of the paper. The study demonstrated that the proposed

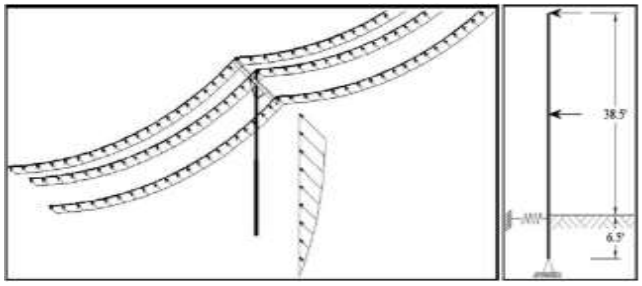

FIGURE 4. The DSN's pole baseline dimension structure [26].

BN-DSN line damage simulated are more accurate DSN line fault prediction when compared with the combined statistical DSN line's FC-MCS-SCENRED predictive model [20], [21]. In [25], the proposed BN-DSN was also applied to a 48-bus DSN to forecast the DSN line's fault scenario leveraging the predicted oncoming hurricane Ewiniar data. The DSN line's damage scenario prediction enhanced the DSO's situational awareness to perform a cost-effective system operational planning against a predictable hurricane event. Therefore, for the readers' clarity, with no intention of repeating an already established concept in our previous papers, the procedural steps for the development of the proposed BN-DSN line fault predictive algorithm were improved and abstractly presented in this section.

To evaluate the reliability or failure probabilities of the DSN components, one ought to consider the reality that the DSN lines can fail due to one or more DSN components' failure. In this paper, it is considered that the power outage in the DSN in a particular area can lead to power supply interruption in another area. This implies that power supply service interruption may be caused by the failure of the DSN components such as poles and overhead wires, due to the dynamic impact of hurricane wind speed intensity across the DSN. Therefore, the study of the DSN pole damage as DSN line fault "causalities" are based on the elasticity perseverance of the DSN poles amid hurricane wind speed intensity (HS) and the DSN poles' foundation's quality that provides resistance to the pole stretch against HS. Due to the unavailability of all the required data about the DSN, the conceivable overhead electrical cable structures are utilized to depict the DSN topology structural reliability as shown in Fig. 4 [26]. Therefore, this proposed DSN line fault predictive model gives a sound premise to the BN-DSN line fault prediction analysis.

Considering the flexural failure points of the DSN lines shown in Fig. 4, both the pole structure and the overhead conductors exposed to the hurricane event would experience the stress of the HS that can possibly result to a pole bending moment, to the ground. In this context, the DSN pole failure under a hurricane event can be expressed as the peak bending moment (BM) shown in (1):

$$M_{\max} = M_p + \sum (M_w + W_w) \tag{1}$$

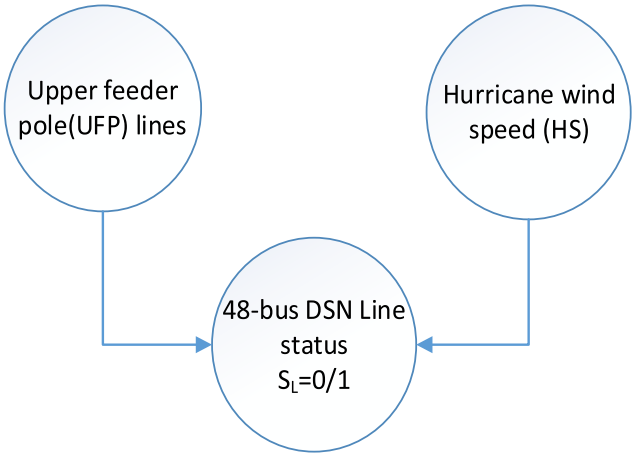

FIGURE 5. The pre-hurricane BN-DSN-DAG model [21].

where M_p is the DSN pole bending moment caused by HS, M_w represents HS induced bending moment of the DSN's conductors, and W_w represents the conductor's span length. The inside strands of the DSN poles are packed and the external filaments are stretched out because of the pole's base bending moment. In case the tensile stress of the extended external fibre surpasses the most extreme pole crack stretch, at that point the DSN pole will be broken. The breaking point state capacity of the flexural failure mode G(x) is introduced in (2) [26].

$$G(x) = R - W = \delta_r - \delta_g = \delta_r - \frac{M_g}{Z} = \delta_r - \frac{32\,M_g}{\pi\,D_{pole}^3} \quad (2)$$

where R is the resistance capacity, W is the wind load, δ_r is the mean modulus of rupture (MOR) of the DSN poles (r), and ground line (δ_g) is the tensile stress of the DSN pole at the ground line, M_g is the bending moment at the ground line, Z represents pole section modulus, and D represents the diameter of the pole at the ground line. The detailed modelling of the designated fibre stress due to HS on various wooden poles in the DSN has been proposed in [27], while the yardstick for quantifying the resilience of the power utility DSN's poles is proposed in [28]. In the BN-DSN model, an all-inclusive CPD related to hurricane event forecast is utilized to define the DSN line fault forecast problem formulation. The failure probabilities (FP) of the DSN lines under hurricane events can be represented by (3) [29], [30].

In the development of the BN-DSN line fault predictive algorithm, two factors were contemplated to be causing the power outages on the DSN lines whenever a hurricane event struck. These factors include the hurricane wind speed (HS) measured in meters per second (m/s), and the situation of the upper feeder pole (UFP) distributing power to the lower feeder pole (LFP) lines. This study utilized these factors to design the proposed BN-directed acyclic graph (BN-DAG) shown in Fig. 5, based on graph theory concept.

A graph theory technique represented by G (N, B) was utilized to evaluate the condition of the 48-bus DSN's lines status when a hurricane event struck. G is the graph, N depicts the DSN's parent (UFP and HS) and child nodes (SL) condition respectively. B on the other hand, represents the DSN link between the parents' nodes and the child node. To estimate the 48-bus DSN line fault's probabilities using the conditional probability distribution (CPD) of Shenzhen region of China, the need to put into consideration the influence of the two independent random and continuous variables of the parents' nodes become imperative. The condition of the two parents' nodes directly affects the child node's status (S_L) as shown in Fig. 5. Therefore, the general term to describe the regional CPD of the hurricane-prone zone under study, that models the DSN line fault prediction is presented in (3) as proposed in [29] and [30], respectively.

$$P_{Fl}^0 = \mathrm{P}(S_L = 0|\mathrm{HS}) \quad (3)$$

where P_{Fl}^0 is the likelihood that the DSN line will be broken or not broken when the hurricane events struck the grid "l" is a subset DSN line of the universal DSN line set "L". S_L depicts the DSN line's condition after the hurricane event (that is $S_L = 0$, or $S_L = 1$). HS represents the hurricane event wind speed data. Therefore, if the probability distribution function (PDF) of the hurricane-prone region and the predicted approaching hurricane data are provided by the weather station, the BN-DSN-DAG model in Fig. 5, can be put in place to predict the maximum likelihood of the DSN line fault. The mathematical expression for this formulation is shown in (4) [29], [30].

$$\mathrm{BN} = \{\mathrm{Nodes_{BN}}, \mathrm{Lines_{BN}}, \mathrm{CPD_{BN}}\} \quad (4)$$

where $\mathrm{Nodes_{BN}} = \{n_i\}, i \in [1, N]$ is the set of random variables described in Fig. 5. $Line_{BN} = \{(n_i, n_j)\}, i \neq j$, represents the edge set, that is, the grid's branch of the proposed BN predictive model. $\mathrm{Lines_{BN}}$ depicts the main causes of the DSN line fault. The two parents and child node relationship are described by the nodes (n_i), and edges ($\boldsymbol{n}$j). For instance, consider n_i, where all its parent nodes and child node are classified as the set of $\pi_{UFP,HS,SL}(n_i)$, therefore a parent node with a known value can be defined as an independent node in a BN-DSN-DAG model. Similarly, the dependent node ($\boldsymbol{n}_j$) that utilizes the hurricane-prone region CPD, represented by θ_{BN}, is also defined in the BN-DSN-DAG model, given that the values of all its parent nodes are provided. The DSN-CPD mathematical expression for the proposed BN-DSN line fault model is presented in (5) [29], [30].

$$\theta_{\mathrm{BN}} = \mathrm{P_F}(n_i \mid \pi_{UFP,HS}(n_i)) \quad (5)$$

In this study, it was assumed that if the dynamic HS across the 48-bus DSN is above 65 m/s (category 4-hurricane event) and it is sustained for more than 60 seconds across the DSN, any DSN pole hit with such HS will be broken, otherwise it will not be broken. In the same vein, if UFP line of the DSN is damaged, no power would be supplied to the LPF lines. These two constraints were used to model the DSN line

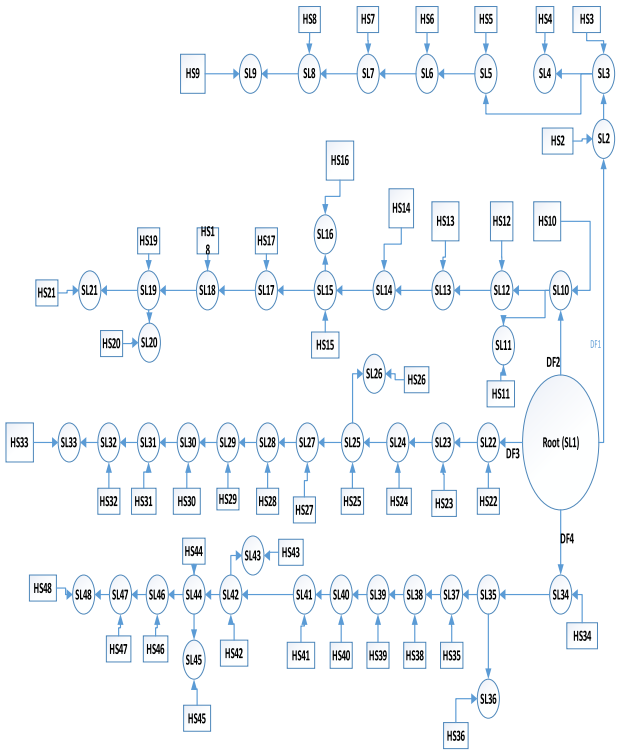

FIGURE 6. Structure of BN-DSN-DAG model for the establishment of 48-bus DSN -CPD [25].

status after a hurricane event. This relationship is presented in (6).

$$\text{Nodes}_{\text{BN}} = \{S_L, \text{HS}\}, \quad l \in L \tag{6}$$

To model the BN-CPD between the HS and the DSN-UFP lines, the past recorded and stored hurricane event data of the Shenzhen region in China was utilized [19]. The goal of the proposed BN-CPD is to generate the DSN line fault probabilities using the CPD of the region under study to model the DSN line damage or not damage conditions. Therefore, using the proposed BN-DSN-DAG model structure in Fig. 5, the 48-bus DSN line fault under the predicted oncoming HS is modeled as presented in Fig. 6.

In Fig. 6, the DSN line 1, (SL1), is the root node (i.e., the transmission bus). SL2, SL10, SL22, and SL34 represent the power supplying distribution feeders (DFs) 1, 2, 3, and 4 respectively. The BN-DSN predictive model mimics the existing relationship between the 48-bus DSN's poles and HS, taking into account the conditional dependence between the DSN parents and child nodes via the DSN branches. This is translated as BN-DSN structure using the region's PDF and the CPD approaches shown in Table 3.

In Table 3, P (SL2 = LB or LNB|HS2) represents the probability that the SL2 "will not be broken" or "will not be broken" given that it is struck by hurricane wind speed intensity 2 (HS2). In the same vein, P (SL3 = LB or LNB|HS3, SL2) means the probability that the SL3 "will be broken" or

TABLE 2. The BN Probability Distribution Function (PDF) and Conditional Probability Distribution (CPD) chart.

$n_i - n_j$ Nodes	PDF / CPD	The DSN line break (LB)	The DSN line did not break (LNB)	The DSN Line break Probabilities (LBP)	The DSN line did not break probabilities (LNBP)
1-2	P(SL2=LB or LNB|HS2)	P(SL2=LB | HS2)	P(SL2=LNB| HS2)	0.012	0.996
2-3	P(SL3=LB or LNB|HS3,SL2)	P(SL3=LB | HS3,SL2)	P(SL3=LNB| HS3, SL2)	0.015	0.994
3-4	P(SL4=LB or LNB|HS4,SL3)	P(SL4=LB|HS4, SL3)	P(SL4=LNB| HS4, SL3)	0.02	0.992
3-5	P(SL5=LB or LNB|HS5,SL3)	P(SL5=LB |HS5,SL3)	P(SL5=LNB| HS5, SL3)	0.025	0.988
5-6	P(SL6=LB or LNB|HS6,SL5)	P(SL6=LB |HS6,SL5)	P(SL6=LNB| HS6, SL5)	0.031	0.984
6-7	P(SL7=LB or LNB|HS7,SL6)	P(SL7=LB |HS7,SL6)	P(SL7= LNB|HS7,SL6)	0.038	0.979
7-8	P(SL8=LB or LNB|HS8,SL7)	P(SL8=LB |HS8,SL7)	P(SL8=LNB| HS8, SL7)	0.046	0.972
8-9	P(SL9=LB or LNB|HS9,SL8)	P(SL9=LB |HS9,SL8)	P(SL9=LNB| HS9, SL8)	0.056	0.964
1-10	P(SL10=LB or LNB|HS10,SL1)	P(SL10=LB| HS10, SL1)	P(SL10=LNB |HS10, SL1)	0.067	0.953
10-11	P(SL11=LB or LNB|HS11,SL10)	P(SL11=LB |HS11,SL10)	P(SL11=LNB |HS11,SL10)	0.08	0.941
10-12	P(SL12=LB or LNB|HS12,SL10)	P(SL12=LB |HS12,SL10)	P(SL12=LNB |HS12, SL10)	0.094	0.926
12-13	P(SL13=LB or LNB|HS13,SL12)	P(SL13=LB |HS13,SL12)	P(SL13=LNB |HS13, SL12)	0.11	0.909
13-14	P(SL14=LB or LNB|HS14,SL13)	P(SL14=LB |HS14,SL13)	P(SL14=LNB |HS14, SL13)	0.128	0.890
14-15	P(SL15=LB or LNB|HS15,SL14)	P(SL15=LB| HS15, SL14)	P(SL15=LNB |HS15, SL14)	0.148	0.868
15-16	P(SL16=LB or LNB|HS16,SL15)	P(SL16=LB |HS16,SL15)	P(SL16=LNB |HS16, SL15)	0.169	0.843

TABLE 2. *(Continued.)* **The BN Probability Distribution Function (PDF) and Conditional Probability Distribution (CPD) chart.**

15-17	P(SL17= LB or LNB|HS 17,SL15)	P(SL17=LB |HS17,SL15)	P(SL17= LNB |HS17, SL15)	0.193	0.816
17-18	P(SL18= LB or LNB|HS 18,SL17)	P(SL18=LB |HS18,SL17)	P(SL18= LNB |HS18, SL17)	0.219	0.787
18-19	P(SL19= LB or LNB|HS 19,SL18)	P(SL19=LB |HS19,SL18)	P(SL19= LNB| HS19, SL18)	0.246	0.755
19-20	P(SL20= LB or LNB|HS 20,SL19)	P(SL20=LB |HS20,SL19)	P(SL20= LNB| HS20, SL19)	0.256	0.722
19-21	P(SL21= LB or LNB|HS 21,SL19)	P(SL21=LB |HS21,SL19)	P(SL21=LNB |HS21, SL19)	0.286	0.687
1-22	P(SL22= LB or LNB|HS 22,SL1)	P(SL22=LB |HS22,SL1)	P(SL22=LNB |HS22, SL1)	0.318	0.650
22-23	P(SL23= LB or LNB|HS 23,SL22)	P(SL23=LB |HS23,SL22)	P(SL23=LNB |HS23, SL22)	0.352	0.613
23-24	P(SL24= LB or LNB|HS 24,SL23)	P(SL24=LB |HS24,SL23)	P(SL24=LNB |HS24, SL23)	0.387	0.575
24-25	P(SL25= LB or LNB|HS 25,SL24)	P(SL25=LB |HS25,SL24)	P(SL25=LNB |HS25, SL24)	0.423	0.537
25-26	P(SL26= LB or LNB|HS 26,SL25)	P(SL26=LB |HS26,SL25)	P(SL26=LNB |HS26, SL25)	0.46	0.498
25-27	P(SL27= LB or LNB|HS 27,SL25)	P(SL27=LB |HS27,SL25)	P(SL27=LNB |HS27, SL25)	0.498	0.460
27-28	P(SL28= LB or LNB|HS 28,SL27)	P(SL28=LB |HS28,SL27)	P(SL28=LNB |HS28, SL27)	0.537	0.423
28-29	P(SL29= LB or LNB|HS 29,SL28)	P(SL29=LB |HS29,SL28)	P(SL29=LNB |HS29, SL28)	0.575	0.387
29-30	P(SL30= LB or LNB|HS 30,SL29)	P(SL30=LB |HS30,SL29)	P(SL30=LNB |HS30, SL29)	0.613	0.352
30-31	P(SL31= LB or LNB|HS 31,SL30)	P(SL31=LB |HS31,SL30)	P(SL31=LNB |HS31, SL30)	0.65	0.318
31-32	P(SL32= LB or LNB|HS 32,SL31)	P(SL32=LB |HS32,SL31)	P(SL32=LNB |HS32, SL31)	0.687	0.286
32-33	P(SL33= LB or LNB|HS 33,SL32)	P(SL33=LB |HS33,SL32)	P(SL33=LNB |HS33, SL32)	0.722	0.256
1-34	P(SL34= LB or LNB|HS 34,SL1)	P(SL34=LB |HS34,SL1)	P(SL34=LNB |HS34, SL1)	0.755	0.246
34-35	P(SL35= LB or LNB|HS 35,SL34)	P(SL35=LB |HS35,SL34)	P(SL35=LNB |HS35, SL34)	0.787	0.219
35-36	P(SL36= LB or LNB|HS 36,SL35)	P(SL36=LB |HS36,SL35)	P(SL36=LNB |HS36, SL35)	0.816	0.193
35-37	P(SL37= LB or LNB|HS 37,SL35)	P(SL37=LB |HS37,SL35)	P(SL37=LNB |HS37, SL35)	0.843	0.169
37-38	P(SL38= LB or LNB|HS 38,SL37)	P(SL38=LB |HS38,SL37)	P(SL38=LNB |HS38, SL37)	0.868	0.148
38-39	P(SL39= LB or LNB|HS 39,SL38)	P(SL39=LB |HS39,SL38)	P(SL39=LNB |HS39, SL38)	0.89	0.128
39-40	P(SL40= LB or LNB|HS 40,SL39)	P(SL40=LB |HS40,SL39)	P(SL40=LNB |HS40, SL39)	0.909	0.110
40-41	P(SL41= LB or LNB|HS 41,SL40)	P(SL41=LB |HS41,SL40)	P(SL41=LNB |HS41, SL40)	0.926	0.094
41-42	P(SL42= LB or LNB|HS 42,SL41)	P(SL42=LB |HS42,SL41)	P(SL42=LNB |HS42, SL41)	0.941	0.080
42-43	P(SL43= LB or LNB|HS 43,SL42)	P(SL43=LB |HS43,SL42)	P(SL43=LNB |HS43,SL42)	0.953	0.067
42-44	P(SL44= LB or LNB|HS 44,SL42)	P(SL44=LB |HS44,SL42)	P(SL44=LNB |HS44, SL42)	0.964	0.056
44-45	P(SL45= LB or LNB|HS 45,SL44)	P(SL45=LB |HS45,SL44)	P(SL45=LNB |HS45, SL44)	0.972	0.046
44-46	P(SL46= LB or LNB|HS 46,SL44)	P(SL46=LB |HS46,SL44)	P(SL46=LNB |HS46, SL44)	0.979	0.038
46-47	P(SL47= LB or LNB|HS 47,SL46)	P(SL47=LB |HS47,SL46)	P(SL47=LNB |HS47, SL46)	0.984	0.031

''will not be broken'' provided that, it is connected to SL2 when it was hit by the HS3. Using this approach, the PDF is computed for each pole in the 48-bus DSN as presented in Table 3. The derived 48-bus DSN poles' failure probabilities under hurricane event are presented in Table 3, and plotted in Fig. 7 respectively. The generated 48-bus DSN pole failure probabilities in Table 3, are then compared with the random numbers generated ranging between 0 and 1. The decision-making condition for the predictive probabilistic failure model states that, if the 48-bus DSN line failure

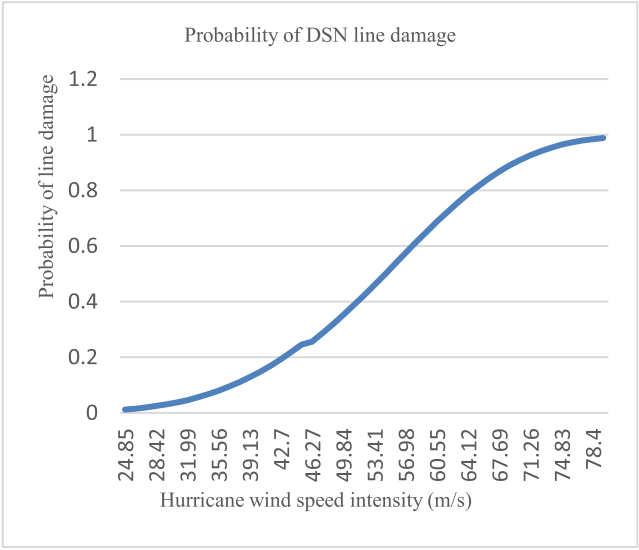

FIGURE 7. The representation of BN-DSN's pole failure probabilities.

probability of each line is less than the random number, the DSN pole is not broken (LNB), otherwise, the DSN pole is broken (LB). This approach is established using Monte Carlo Simulation (MCS) algorithm to generate the 48-bus DSN line fault scenarios data. The data is used alongside with the historical hurricane event data to train the proposed BN-DSN predictive model for future DSN line fault prediction. The mathematical expression for the data set D_{HS} is presented in (7).

$$D_{\mathrm{HS}} = \{S_L, \mathrm{HS}\}\ l \in [1, L], 1 \in [1, \mathrm{HS}] \tag{7}$$

To ascertain the CPD of the 48-bus DSN lines, the softmax approach presented in (8) is employed to handle both the discrete and continuous parents' nodes of Figs. 5 and 6 [31].

$$\mathrm{P}_r(\mathrm{S}_{DSN} = \mathrm{V}|\mathrm{UFP},\mathrm{HS}) = \frac{\ell^{(w^l_{V,UFP} \times UFP + w^L_{V,HS} \times HS + b^l_V)}}{\sum_{V\in(0,1)} \ell^{(w^l_{V,UFP} \times UFP + w^l_{V,UFP} \times HS + b^l_V)}} \tag{8}$$

where $\mathrm{V} \in \{0, 1\}$ is the DSN line condition. The $W^l_{V,p} \in \Re^{1\times 1}, V = 0, 1$ are the DSN line conditions based on the DSN line's UFP. The$W^l_{V,HS} \in \Re^{N\times 1}$ represents the relative weight of the normal vector for the HS within the 48-bus DSN, and b^l_V depicts softmax offset. The relative weight and the biases/offset of the softmax in (8) is defined by (9) as indeterminate parameters of the 48-bus DSN line "l" [31].

$$\varnothing_l = \left\{w^l_{V,UFP}, w^l_{V,HS}, b^l_V\right\}, V \in \{0, 1\} \tag{9}$$

For every DSN line "l," in the 48-bus DSN, $\emptyset_l$ determines their CPD. Also, $\emptyset_l$ can be expressed in term of the BN-DSN predictive model undefined parameters as provided in (10):

$$\varnothing_l \{\varnothing_l | l \in L\} \tag{10}$$

The BN-DSN predictive model's training goal is to determine the DSN's optimal CPDs represented by $\ominus^*_{\mathrm{BN}}$. The optimal learning process is carried out using the offline stored data set in (7). The 48-bus DSN's optimal learning problem formulation is presented in (11) [29], [30].

$$\ominus^*_{\mathrm{BN}} = arg_{\ominus_{BN}}\ max\, P_r\ (\mathrm{D_{HS}} \,|\, \mathrm{Nodes_{BN}}, \mathrm{Line_{BN}}, CPD_{\mathrm{BN}}) \tag{11}$$

Therefore the $\ominus^*_{\mathrm{BN}}$ problem formulation of (11) can then be written in terms of ϕ^* as shown in (12) [29], [30].

$$\phi^* = arg_{\ominus_{BN}}\ max\, P_r\ (\mathrm{D_{HS}} \,|\, \mathrm{Nodes_{BN}}, \mathrm{Line_{BN}}, CPD_{BN}) \tag{12}$$

The criterion of (11) can be learned by the use of a gradient-descent algorithm, given that the actual mastering rate of $\eta \in (0,1)$ are provided and the initial value of the optimal CPDs of $\phi^{(0)}$ is known. Subsequently, after a few simulations, the parameter of the BN-DSN predictive model will accomplish convergence based on the guideline of maximum probability assessment of the preparing data set. At this stage, the complete proposed BN-DSN line fault predictive algorithm is presented as a joint probability distribution (JPD) using the 48-bus DSN nodes ($Nodes_{BN}$). The BN-DAG random variables from Fig. 5 are presented, using (13), [29], [30].

$$\mathrm{BN} \Leftrightarrow \mathrm{P_r(S,HS)} \tag{13}$$

where $\mathrm{S} = \{S_L l \in [1, L]\}$, S_L represents the vector quantity with binary values of 0 and 1 showing the whole system line status after the hurricane event. S represents the whole scenarios of the 48-bus DSN line status. Therefore, the CPD of the random variables for the 48-bus DSN line status (S) is given by (14), [29], [30].

$$\begin{aligned}\mathrm{P}_r(\mathrm{S}|\mathrm{HS}) &= \prod_{l=1}^{L} P_r(S_l \,|\, \pi_{(UFP,HS)}\, BN(S_l)) \\ &=\in \prod_{l=1}^{L} P_r(S_l \,|UFP, HS)\end{aligned} \tag{14}$$

where $HS = [HS_1 \ldots, HS_l \ldots, HS_L]$ is the set of hurricane speeds across the 48-bus DSN. Equation (14) is assessed with the hurricane Ewiniar prediction data to determine the likelihood of the hurricane event occurrence and the range of the 48-bus DSN line damage. Therefore, the BN-DSN line fault model estimates the DSN line status based on the rule of highest probability of the DSN line fault when the forecasted oncoming hurricane event struck the grid as given in (15), [29], [30].

$$\mathrm{S}^* = \arg_S \max P_r(\mathrm{S}|\mathrm{HS}) = \arg_S \max P_r(S|HS) \tag{15}$$

where S^* represents the 48-DSN line fault range. S^* is also the DSN line fault prediction results presented in terms of LB or LNB in this study or better presented as $S_l = 0\ or\ S_l = 1$, that is 0 means line damage, and 1 means otherwise. The proposed BN-DSN predictive model is implemented on

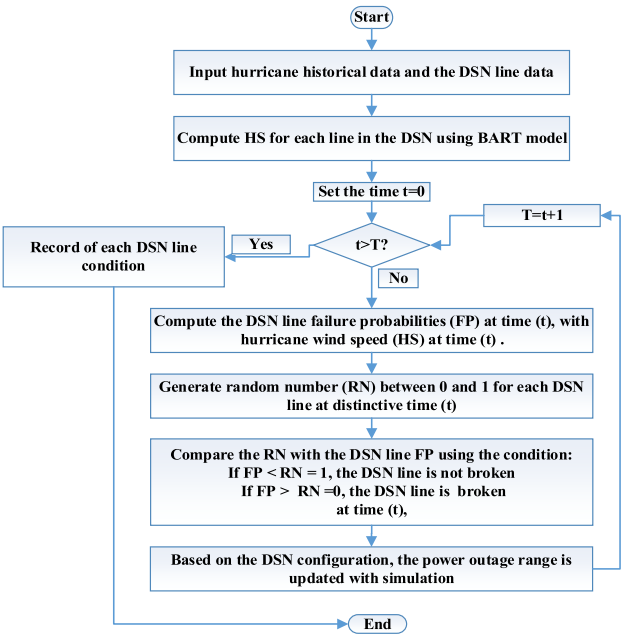

FIGURE 8. The BN-DSN line fault prediction simulation flowchart on the DSN [21].

TABLE 3. BN-DSN line fault prediction for the 48-bus DSN.

BN-DSN prediction	DSN broken lines
Predicted line fault scenario	(27-28), (28-29), (31-32), (32-33), (1-34), (34-35), (35-36), (35-37), (37-38), (39-40), (40-41), (41-42), (42-43), (44-45), (44-46), (46-47), (47-48).

the modified 48-bus DSN using the CPD of the proposed BN-DSN-DAG predictive algorithm. The hurricane-induced power system line fault prediction was carried out using Hurricane Ewiniar data [32], with its corresponding simulated system line fault scenario. The BN-DSN predictive model program written with MATLAB toolbox by Murphy in [31] and [33] was studied and modified using R program [34], to suit our BN-DSN line faults prediction goal. The detailed algorithm flow chart for the BN-DSN line fault simulation is presented in Fig. 8. The resulting 48-bus DSN line fault prediction under hurricane Ewiniar is presented in Table 3.

2) MODELING OF THE PROPOSED HYBRID STATISTICAL DSN LINE'S FC-MCS-SCENRED LINE DAMAGE PREDICTIVE ALGORITHM FOR THE PREDICTED ONCOMING HURRICANE EVENT

To model the proposed combined statistical DSN line's FC-MCS-SCENRED predictive algorithm, it is important to keep in mind the same condition considered in (1) and (2) respectively. Having stated this fact, our past work that presents the detailed procedural steps for the development of the proposed combined statistical DSN line's FC-MCS-SCENRED predictive model can be found in [20]. However,

TABLE 4. Statistical approach to pole's failure probability caused by anticipated HS.

y	m	x	b
$\ln\left(\ln\left(\frac{1}{1-P_F(\sigma)}\right)\right)$	m	$\ln\sigma$	$-m\ln\sigma_0$

for readers' convenience, this concept is abstractly presented in this section using a modified 48-bus DSN.

The DSN's wooden pole and conductor are considered for this investigation. The first task is to establish the risk of a wooden pole's failure under HS and scale this risk over the DSN configuration as displayed in Fig. 4. The DSN maximum bending moment under HS is defined by (1) [26]. According to the rule of structural reliability in Civil Engineering field, which states that if electric pole cracks caused by an extreme weather condition are distributed within the component, as component's failure probabilities, the crack propagation of the DSN pole can eventually cause the electric line to fail under extreme weather conditions causing a large-scale power blackout [35]. Therefore, the DSN pole failure probabilities under hurricane events were modelled as presented in (16) [36], [37].

$$\mathrm{P_F}(\sigma) = 1 - \mathrm{e}^{-\left(\frac{\sigma}{\sigma 0}\right)^{\mathrm{m}}} = P_F^L\left(H_l^{HS}\right) \tag{16}$$

where, $\mathrm{P_F}(\sigma)$ is the electric pole probability of failure, as a function of failure stress(σ) of HS. σ_0, represents the reference pole stretch under HS, and m represents the statistical Weibull modulus. Both (σ_0, m) are calculated from the available historical hurricane data. Given historical hurricane Ewiniar data, the zonal HS, PDF, CDF, and the redesigned 48-bus DSN poles failure probabilities are calculated by rewritten (16) to obtain (17) [38].

$$1 - P_F(\sigma) = \mathrm{e}^{-\left(\frac{\sigma}{\sigma 0}\right)^{\mathrm{m}}} \tag{17}$$

By taking the log of both sides of (17), (18) is obtained.

$$\mathrm{m}\ln\left(\frac{\sigma}{\sigma 0}\right) = \ln\left(\ln\frac{1}{(1-P_F(\sigma))}\right) \tag{18}$$

Equation (18) is presented as a straight-line equation, in the form of $y = mx + b$ shown in (19). The breakdown is presented in Table 4.

$$\ln\left(\ln\left(\frac{1}{1-P_F(\sigma)}\right)\right) = \mathrm{m}\ln\sigma - \mathrm{m}\ln\sigma_0 \tag{19}$$

It was modeled such that the HS that passed through the 48-bus DSN began to stress the DSN's poles from hurricane wind speed of 24.85 ms^{-1} to 79.59 ms^{-1}, and at 80 ms^{-1} and above, the pole starts to fail. The corresponding DSN line's failure probabilities is presented in Fig. 9, having duly considered the impact of hurricane wind speed's PDF and CPD of the region under study. The Statistical Weibull parameters of slope m = 3.862 and σ_O= 60.958, derived from (16) were used for graph plotting shown in Fig. 9.

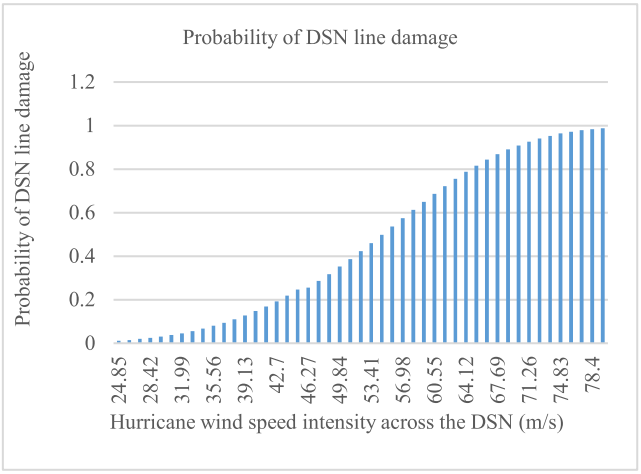

FIGURE 9. The 48-bus DSN line's failure probabilities under hurricane event.

Using (16), the redesigned 48-bus DSN's poles failure probabilities due to HS are obtained. The data is then compared with their corresponding generated random numbers (r_n) ranging between 0 and 1 ($r_n \sim 0, 1$), (See Table 5). The rule that determines the condition of the redesigned 48-bus DSN line status as presented in (20), states that, if each generated random number for each DSN line is compared with its corresponding DSN's line failure probabilities under a hurricane event, and the random number is less than the DSN pole's failure probabilities, the line is damaged "1", otherwise the line is not damaged "0" [39]. But in this article, "0", is used to represent line fault while "1" is used to represent DSN line, not damage. This is the condition used to model this combined statistical DSN line's FC-MCS-SCENRED predictive algorithm.

$$P_F^L\left(H_l^{HS}\right) = \begin{cases} 0, & \text{if } r_n < \mathrm{P_F}(I) \\ 1, & \text{if } r_n > \mathrm{P_F}(I) \end{cases} \tag{20}$$

where $P_F^L\left(H_l^{HS}\right) = 0$ is the likelihood that the redesigned 48-bus DSN lines will fail or be broken, whereas when $P_F^L(H_l^{HS}) = 1$ is the likelihood that the redesigned 48-bus DSN lines will not fail or will not be broken.

In the same vein, due to the need to take into account the probabilistic nature of the hurricane event across the redesigned 48-bus DSN, the MCS model is employed to forecast the possible DSN line fault scenarios due to hurricane Ewiniar [40]. The MCS has been employed in many studies in the past without defining proper stopping criteria. This usually affects its prediction accuracy since there are no universally accepted stopping criteria currently [22]. However, some studies such as [18] and [39], in power system resilience, claimed that 1000 DSN line fault scenarios prediction from the MCS model is enough to guarantee power system line fault prediction accuracy under extreme weather events like hurricane events. Therefore, 1000 MCS line fault prediction is adopted in this study. In this view, the DSN line fault prediction was simulated using the redesigned 48–bus DSN, on an excel spreadsheet. The samples of the redesigned 48–bus DSN line fault prediction from the DSN line's FC-MCS model is shown in Table 5. Each DSN line fault prediction scenario represents the system line status and the DSN's response to the hurricane events. It should be noted that the combined statistic stochastic system optimization simulation result's accuracy largely depends on the higher number of the DSN line fault scenarios generated from the predictive statistical DSN line's FC-MCS model. Alas, these higher DSN line fault scenarios generated usually result in computational high time costs when the generated large numbers of system line fault scenarios are used to perform stochastic system optimization simulation. In this context, one of the ways around this problem of computational time cost is to apply the scenario reduction (SCENRED) algorithm to the modified 48-bus DSN's 1000 line fault prediction scenarios. This is to reduce the generated system line fault scenarios to a smaller desired number of the DSN line fault scenarios without jeopardizing the precision of the predicted DSN line damages scenarios [20]. The reduced DSN line fault scenarios are then used to perform the pre-hurricane events stochastic system optimization [41]. The developed SCENRED program in GAMS [42], was applied to the modified 48-bus DSN line damages scenarios predicted from combined statistical DSN's line FC-MCS model, to reduce its predicted 1000-line fault scenarios to 10 with their corresponding optimum probabilities of system line fault for each reduced system line fault scenario generated. See Table 6 for the 10 reduced DSN line fault scenarios.

III. DISCUSSION ON THE PROPOSED BN-DSN AND HYBRID STATISTICAL DSN'S LINE FAULT PREDICTION MODELS

The efficiency of the proposed predictive BN-DSN and the combined statistical DSN line's FC-MCS-SCENRED predictive models under hurricane events was studied through the DSN line fault simulation on the 48-bus DSN. In both cases, the algorithm solvers depend on adaptive search techniques, particularly, the Branch-and-Bound method [43]. So, the closeness in the prediction time and memory as presented in Table 7, is not surprising because of the hybridization of SCENRED algorithm to the combined statistical DSN line's FC-MCS model. The improved statistical predictive algorithm optimally reduces the system line fault prediction to a small sizable number without jeopardizing the system line fault prediction accuracy [41], [44]. Comparing the DSN line fault prediction time and computer memory usage in both predictive algorithms as shown in Table 7, the proposed predictive BN-DSN line fault model still predicted the DSN line fault scenario faster because it works based on the principle of predicting the maximum probability of DSN line fault based on the predicted oncoming hurricane event when compared to the combined statistical DSN line's FC-MCS-SCENRED model, justifying the efficacy of the proposed BN-DSN model over all the existing combined statistical DSN line's

TABLE 5. Statistical approach to pole's failure probability caused by anticipated HS.

Lines ($n_i - n_j$)	FP	Random no1	Random no2	Random no3
1 to 2	0.012	0.396482	0.273657	0.571337
2 to 3	0.015	0.767989	0.069451	0.525599
3 to 4	0.020	0.985294	0.443266	0.821186
3 to 5	0.025	0.442897	0.542141	0.096017
5 to 6	0.031	0.410355	0.712613	0.345207
6 to 7	0.038	0.866693	0.173840	0.928005
7 to 8	0.046	0.762788	0.636939	0.637332
8 to 9	0.056	0.600936	0.051771	0.278518
1 to 10	0.067	0.866129	0.567419	0.798554
10 to 11	0.080	0.809320	0.055593	0.009207
10 to12	0.094	0.787691	0.911512	0.496573
12 to 13	0.110	0.421445	0.935480	0.832852
13 to 14	0.128	0.092215	0.441247	0.154671
14 to 15	0.148	0.537253	0.349505	0.737580
15 to 16	0.169	0.176553	0.672768	0.789073
15 to17	0.193	0.596964	0.208077	0.844851
17 to 18	0.219	0.225397	0.074382	0.815725
18 to 19	0.246	0.895751	0.232241	0.253087
19 to 20	0.256	0.638648	0.580942	0.568003
19 to 21	0.286	0.637767	0.510698	0.399450
1 to 22	0.318	0.752264	0.673494	0.718061
22to23	0.352	0.873969	0.435633	0.021573
23 to 24	0.387	0.991544	0.053092	0.561994
24 to 25	0.423	0.784078	0.857966	0.985714
25 to 26	0.460	0.844299	0.083749	0.586260
25 to 27	0.498	0.864497	0.974337	0.155331
27 to 28	0.537	0.370596	0.300191	0.967459
28 to 29	0.575	0.001511	0.276535	0.229493
29 to 30	0.613	0.064965	0.708876	0.750348
30 to 31	0.650	0.179330	0.147241	0.069561
31 to 32	0.687	0.664618	0.311244	0.185435
32 to 33	0.722	0.993052	0.021091	0.037383
1 to 34	0.755	0.665305	0.243131	0.969438
34 to 35	0.787	0.876753	0.870564	0.621826
35 to 36	0.816	0.555383	0.463705	0.228275
35 to 37	0.843	0.080781	0.456347	0.061954
37 to 38	0.868	0.250396	0.201889	0.625136
38 to 39	0.890	0.544382	0.612429	0.347544
39 to 40	0.909	0.360260	0.834761	0.847717
40 to 41	0.926	0.184402	0.773201	0.625509
41 to 42	0.941	0.714329	0.504332	0.876747
42 to 43	0.953	0.276859	0.945783	0.449301
42 to 44	0.964	0.113542	0.122391	0.024760
44 to 45	0.972	0.770835	0.333847	0.325078
44 to 46	0.979	0.555497	0.430080	0.858802
46 to 47	0.984	0.061245	0.064176	0.371160
47 to 48	0.988	0.096154	0.034434	0.012441

HS(m/s)	Lines ($n_i - n_j$)	Damage scenario1	Damage scenario2	Damage scenario3
24.85	1 to 2	1	1	1
26.04	2 to 3	1	1	1
27.23	3 to 4	1	1	1
28.42	3 to 5	1	1	1
29.61	5 to 6	1	1	1
30.80	6 to 7	1	1	1
31.99	7 to 8	1	1	1
33.18	8 to 9	1	0	1
34.37	1 to 10	1	1	1
35.56	10 to 11	1	0	0
36.75	10 to12	1	1	1
37.94	12 to 13	1	1	1
39.13	13 to 14	0	1	1
40.32	14 to 15	1	1	1
41.51	15 to 16	1	1	1
42.70	15 to17	1	1	1
43.89	17 to 18	1	0	1
45.08	18 to 19	1	0	1
46.27	19 to 20	1	1	1
47.46	19 to 21	1	1	1
48.65	1 to 22	1	1	1
49.84	22to23	1	1	0
51.03	23 to 24	1	0	1
52.22	24 to 25	1	1	1
53.41	25 to 26	1	0	1
54.60	25 to 27	1	1	0
55.79	27 to 28	0	0	1
56.98	28 to 29	0	0	0
58.17	29 to 30	0	1	1
59.36	30 to 31	0	0	0
60.55	31 to 32	0	0	0
61.74	32 to 33	1	0	0
62.93	1 to 34	0	0	1
64.12	34 to 35	1	1	0
65.31	35 to 36	0	0	0
66.50	35 to 37	0	0	0
67.69	37 to 38	0	0	0
68.88	38 to 39	0	0	0
70.07	39 to 40	0	0	0
71.26	40 to 41	0	0	0
72.45	41 to 42	0	0	0
73.64	42 to 43	0	0	0
74.83	42 to 44	0	0	0
76.02	44 to 45	0	0	0
77.21	44 to 46	0	0	0
78.40	46 to 47	0	0	0
79.59	47 to 48	0	0	0

FC-MCS-SCENRED predictive model. The accuracy of both the proposed DSN line fault predictive algorithms can be confirmed as the scenario 7 of Table 6, which recorded the highest probability of DSN line fault scenario to occur, if a hurricane event struck the DSN, matched the single line fault prediction scenario in Table 3. The detailed explanation of prediction accuracy analysis can be found in [21] and [25].

The predicted DSN line's fault scenarios from both the predictive algorithms under hurricane event are leveraged, by the DSO as power system resilience proactive operational planning tool to decrease the expected load loss. In this context, the pre-hurricane event DSN optimization problems were formulated based on the two predicted DSN line fault scenarios. The impact of the two predictive algorithms was quantified and compared using minimization of the expected load loss as the resilience metric. The modelling of the pre-event DSN optimization is detailed in the next section.

IV. PRE-HURRICANE EVENT DSN RECONFIGURATION AND RESOURCES PLANNING FOR RESILIENCE IMPROVEMENT

The review of system network reconfiguration methodologies presented in [17], [22], and [45] provide a guide in choosing the most appropriate DSN reconfiguration optimization problem formulation approach employed in this study. Morelato and Monticelli [46], revealed that due to the magnitude and non-linear nature of the DSN, a combination of system optimization and heuristic approaches could not achieve an optimal solution [46]. It then suggested that, since it is possible to linearize the pair of objective function and the system

TABLE 6. The 10 reduced Statistical System Line fault Prediction Scenarios.

Scenarios	Reduced predicted 48-bus DSN line damages scenarios	Prob. of event occurrence
Sc 1	(24-25), (27-28), (28-29), (31-32), (32-33), (1-34), (34-35), (35-36),(35-37),(37-38), (39-40), (40-41), (41-42),(42-43),(44-45), (44-46), (46-47), (47-48)	0.1210
Sc 2	(1-22),(22-23),(25-26),(27-28),(29-30), (31-32),(32-33),(1-34),(34-35),(35-36), (35-37),(37-38),(39-40),(40-41),(41-42), (42-43),(44-45),(44-46), (46-47),(47-48)	0.0520
Sc 3	(22-23),(25-26),(27-28),(29-30),(31-32), (1-34),(34-35),(35-36),(35-37),(37-38), (39-40),(40-41),(41-42),(42-43),(44-45), (44-46),(46-47),(47-48)	0.0600
Sc 4	(1-22),(27-28),(28-29),(29-30),(31-32), (32-33),(1-34),(34-35),(35-36),(35-37), (37-38),(39-40),(40-41),(41-42),(42-43), (44-45),(44-46),(46-47),(47-48)	0.1510
Sc 5	(22-23),(24-25),(29-30),(31-32),(32-33), (1-34),(34-35),(35-36),(35-37),(37-38), (39-40),(40-41),(41-42),(42-43),(44-45), (44-46),(46-47),(47-48)	0.1450
Sc 6	(19-20),(19-21),(24-25),(25-26),(28-29), (31-32),(32-33),(1-34),(34-35),(35-36), (35-37),(37-38),(39-40),(40-41),(41-42), (42-43),(44-45),(44-46),(46-47),(47-48)	0.0630
Sc 7	(27-28),(28-29),(31-32),(32-33),(1-34), (34-35),(35-36),(35-37),(37-38),(39-40), (40-41),(41-42),(42-43),(44-45),(44-46), (46-47),(47-48)	0.1570
Sc 8	(23-24),(27-28),(28-29),(29-30),(31-32), (32-33),(1-34),(34-35),(35-36), (35-37), (37-38),(39-40),(40-41),(41-42),(42-43), (44-45),(44-46), (46-47), (47-48)	0.0570
Sc 9	(23-24),(27-28),(28-29),(31-32),(32-33), (1-34), (34-35),(35-36),(35-37),(37-38), (39-40),(40-41),(41-42),(42-43),(44-45), (44-46),(46-47), (47-48),(21-30),	0.0960
Sc10	(19-20),(25-26),(27-28),(28-29),(29-30), (31-32),(32-33),(1-34),(34-35),(35-36), (35-37),(37-38),(39-40),(40-41),(41-42), (42-43),(44-45),(44-46),(46-47),(47-48)	0.0790

TABLE 7. The comparative analysis of the BN-DSN and combined statistical DSN line's FC-MCS-SCENRED predictive models.

Modified 48-bus line failure anticipating model	Algorithm simulation time (sec.)	Computer memory usage (MB)
Bayesian model (BN)	13.625	16
DSN's line-FC-MCS-SCENRED model	14.968	22

operational constraints, to change the non-linear nature of the DSN reconfiguration problem to a MILP system optimization [45], [47], the MILP problem formulation approach was a choice employed in this paper. The prospective optimal DSN reconfiguration and resource allocation MILP problem formulations were employed to conduct a performance-based comparative study to determine the prospective predictive algorithm that is most appropriate to execute pre-hurricane event DSN operational planning in the future. The formulated MILP optimization problems in the two cases, were solved using a CPLEX optimizer in GAMS. The DSN optimization solution proposed in this paper drew its inspiration from the pre-hurricane event DSN optimization problem formulated as the crew dispatch and transportation problem in [18], the pre-and post-event system optimization under hurricane event in [48] and [49], and the prospective two-stages system optimization under hurricane event in [50] respectively.

A. PRE-HURRICANE EVENT DSN OPTIMIZATION PROBLEMS FORMULATION USING PREDICTIVE DSN'S LINE FC-MCS-SCENRED AND BN-DSN PREDICTIVE MODELS

Based on the predicted 48-bus DSN line fault scenarios from the prospective combined DSN line's FC-MCS-SCENRED model, and BN-DSN model, the DSO proactively optimizes the DSN operation to obtain the best optimal network reconfiguration for proactive network reconfiguration and DER planning using optimal switching. These actions are aimed at proactively minimizing the value of the expected load loss (MW). The redesigned 48-bus DSN optimization simulations were performed considering the BN-DSN line fault scenario of Table 3 in (22) and all the reduced 10 predicted system line fault scenarios in Table 6 in (21). The prospective formulated system optimization problems are formulated as a MILP problem in (21) and (22) respectively.

$$Min\ OF = Min \sum_{lds=10}^{lds} \sum_{\forall t} \sum_{\forall x} P_{pre}^{lds} \times w_x^F \times E\,P_{lds,x}^{LS} \times dt \tag{21}$$

$$Min\ OF = Min \sum_{t,x} P_{pre}^{eo} \times \omega_F^x \times E\,P_{t,x}^{LS} \times dt \tag{22}$$

Equations (21) and (22) are subjected to the following operational constraints one after the other.

To ensure balanced power flow, the real and reactive power flow within the redesigned 48-bus DSN at a time "t" are modelled as (23) and (24),

$$P_{t,x}^{D} - \left(P_{out@t,x}^{DG} + P_{out@t,x}^{PV} + P_{out@t,x}^{WT} + P_{out@t,x}^{Sub}\right) + \sum_{t} \sum_{l} P_{t,l}^{AC_{flow}} = 0, \forall x, t \tag{23}$$

$$Q_{t,x}^{D} - \left(Q_{out@t,x}^{DG} + Q_{out@t,x}^{PV} + Q_{out@t,x}^{WT} + Q_{out@t,x}^{Sub}\right) + \sum_{t} \sum_{l} Q_{t,l}^{AC_{flow}} = 0, \forall x, t \tag{24}$$

where $P_{t,x}^{D}$ *and* $Q_{t,x}^{D}$ are the active and reactive power demand at the bus "x" at a time "t". $P_{out@t,x}^{DG}$ and $Q_{out@t,x}^{DG}$, $P_{out@t,x}^{PV}$ and $Q_{out@t,x}^{PV}$, and $P_{out@t,x}^{WT}$ and $Q_{out@t,x}^{WT}$ are the active and reactive power output of the distributed energy resources injected at the bus "x", time "t". $P_{t,x}^{Sub}$ *and* $Q_{t,x}^{Sub}$ are variables that indicate the active and reactive power injected from the

transmission line, while

$$\sum_{t}\sum_{l} P_{t,l}^{AC_{flow}} \; and \; \sum_{t}\sum_{l} Q_{t,l}^{AC_{flow}}$$

represent the active and reactive power flowing in the grid lines (l), at time "t".

To ensure that the power that is flowing through a line does not exceed the DSN line's power flow carrying capacity, constraint (25) is employed.

$$-S_{w(t,l)}\, L_{cap(l)} \le P_{t,l}^{AC_{flow}} \le S_{w(t,l)}\, L_{cap(l)}, \forall t, l \tag{25}$$

Constraints (26) and (27) are based on the Distflow model of a linear AC power flow proposed in [51]. Constraints (26) and (27) are relaxed through the big-M technique [52], provided all other attached lines to the bus "x" are in the open state to adhere to network operational constraints [53]. An explanation of how the big-M technique is utilized to relax the constraints in (26) and (27) can be found in [52].

$$V_{t,y} - V_{t,x} + \frac{\left(R_l\, P_{t,l}^{AC_{flow}} + X_l Q_{t,l}^{AC_{flow}}\right)}{\left(V_{t,l}\right)} \ge \left(S_{w(t,l)} - 1\right) M, \;\; \forall t, l \tag{26}$$

$$V_{t,y} - V_{t,x} + \frac{\left(R_l\, P_{t,l}^{AC_{flow}} + X_l Q_{t,l}^{AC_{flow}}\right)}{\left(V_{t,l}\right)} \le \left(1 - S_{w(t,l)}\right) M, \;\; \forall t, l \tag{27}$$

In making sure that the magnitude of voltage experienced at all buses of the redesigned 48-bus DSN is within the normal operating range, constraint (28) is employed.

$$V_{min} \le \mid V_{t,x} \mid \le V_{max}, \quad \forall x, t \tag{28}$$

To ensure that the maximum capacity limit of complex power flowing in a line's is within the line operating limit, (29) is used. Also, to maintain the linearity of the model, the special-ordered-sets-of-type 2 (SOS2) approach is employed to linearize (29), [54].

$$\left(S_{comp}\right)^2 \ge \left(\sum_{t,l} P_{t,l}^{AC_{flow}}\right)^2 + \left(\sum_{t,l} Q_{t,l}^{AC_{flow}}\right)^2 \quad \forall t, l \tag{29}$$

The power output ranges for the DGs, the PV, and the WTs are modelled with the consideration that the PV and WTs are environmental time-varying solar irradiation and wind speed dependent energy-generating components. Therefore, this study assumed that the WTs and PV have a constant power factor, and that the power output sources are P-Q sources. Constraints (30) and (31) are utilized to design the real and reactive power output bound of the DG units.

$$\delta_{t,x}\, P_{min,x}^{DG} \le P_{out@t,x}^{DG} \le \delta_{t,x}\, P_{max,x}^{DG} \quad \forall t, x \tag{30}$$

$$\delta_{t,x}\, Q_{min,x}^{DG} \le Q_{out@t,x}^{DG} \le \delta_{t,x}\, Q_{max,x}^{DG} \quad \forall t, x \tag{31}$$

Furthermore, (32) and (33) ensure that the output power of the photovoltaic panel and the wind turbine units did not exceed their respective maximum power output limits.

$$0 \le P_{out@t,x}^{PV} \le P_{max,t,x}^{PV} \quad \forall t, x \tag{32}$$

$$0 \le P_{out@t,x}^{WT} \le P_{max,t,x}^{WT} \quad \forall t, x \tag{33}$$

To ensure that the DSN is kept in a radial configuration, the constraint proposed in [55], the spanning-tree approach for the power system network analysis is employed for (34), (35), and (36) respectively. The constraints make sure that line "l'' at a time "t" in the spanning tree structure is kept in a radial configuration. That is, $S_{w(t,l)} = 1$, if either of $\gamma_{x,y,t} or \gamma_{y,x,t} = 1$. This implies that when $\gamma_{y,x,t} = 1$, "y" represents the parent bus of "x" at a time "t", and when $\gamma_{x,y,t} = 1$ "x" is the parent bus of "y" at a time "t" respectively.

$$\gamma_{x,y,t} + \gamma_{y,x,t} = S_{w(t,l)} \quad \forall l \in (x, y), y \in \varphi_x, t = E_F \tag{34}$$

$$\sum_{y \in \varphi_x} \gamma_{x,y,t} = 1, \quad \forall y \in \varphi_x, t = E_F \tag{35}$$

$$\sum_{y \in \varphi_x} \gamma_{1,y,t} = 0, \quad \forall y \in \varphi_{root}, t = E_F \tag{36}$$

To put in check the number of times the RCS status changes, constraint (37) is introduced. If the switch status changes for line "l" at a time "t", the binary variable $RCS_{sw(t,l)}$ will be 1, otherwise 0.

$$\sum_{t} RCS_{Sw(t,l)} \le 1, \forall t, l \tag{37}$$

The change in switch status can be detected using, constraints (38) and (39) respectively.

$$-RCS_{Sw(t,l)} \le S_{w(t,l)} - S_{w(t-1,\,l)} \le RCS_{Sw(t,l)} \quad \forall t, l \tag{38}$$

$$RCS_{Sw(t,l)} \le S_{w(t,l)} + S_{w(t-1,l)} \le -RCS_{Sw(t,l)} \quad \forall t, l \tag{39}$$

The time limit to operate the RCSs before hurricane event can be mathematically formulated as (40) and (41) respectively. That is the RCS actions to optimally reconfigure the network modelled in (40) must be performed under the bound of (41), otherwise the pre-hurricane event optimal DSN and resource scheduling will be defeated.

$$\sum_{t} t \times RCS_{Sw(t,l)} \ge RCS_{T,} \quad \forall l \in Sw_l^{RCS} \tag{40}$$

$$\sum_{t} t \times RCS_{Sw(t,l)} \le E_F, \quad \forall l \in Sw_l^{RCS} \tag{41}$$

The DSN optimization problems formulated in MILP method in this section, are solved using a CPLEX solver in the GAMS, making use of a branch and bound algorithm. The solution encourages the deployment of specially ordered sets of variables SOS1, SOS2, semi-continuous, and semi-integer variables proposed in [56]. The algorithm also provides a detailed technique to solve a linearized MILP problem by modifying the constraints in the state-space search approach [43]. It is worth to note that the following assumptions were made prior to the formulation of the pre-hurricane DSN optimization problems:

TABLE 8. System performance loss function (MWh) metrics.

System phase/ equation	HILL events at each phase	Time frame (H)	Areas Under Operational Resilience $SL_{Fi}(I)$ (MWh)
I	System initial degradation state	$(t \in \|[t_{oe}, t_{ee}]\|)$	$SL_{lol\,1}(I) = \frac{1}{2} LoL_1(I)[(t_{ee}, t_{ee})]$
II	Pre-disturbance state.	$(t \in \|[t_{ee}, t_{or}]\|)$	$SL_{lol\,2}(I) = LoL_2(I)[(t_{or}, t_{ee})]$
III	BN-based operational restoration state.	$(t \in \|[t_{or}, T_{or}]\|)$	$SL_{lol\,3}(I) = \frac{1}{2} LoL_3(I)[(T_{or} - t_{or})]$

Total system Loss of loads function = $\int_{t_{oe}}^{t_{ir}} R_{operational}(t)\,dt$

1) All switches are remote-controlled switches.
2) The distributed energy resources (DERs) have been optimally placed in the redesigned 48-bus DSN [24]. Therefore, problems related to voltage fluctuation from the DERs are ignored in this paper.
3) It was assumed that the forecasted oncoming hurricane event is to hit the 48-bus DSN in 60 minutes ahead.

B. THE MILP SIMULATION PLATFORM

The MILP model is fed with the detailed redesigned 48-bus DSN data, remotely controlled switches locations, and predicted DSN line-fault scenarios from both the prospective predictive algorithms. The proposed formulated MILP optimization simulation constraints described in Section IV-A, are used to perform the two cases of pre-hurricane event DSN optimization simulations. The next section describes the system resilience metrics adopted for the simulation results analysis.

C. THE SYSTEM RESILIENCE METRICS

The resilience metrics proposed in [39], shown in Table 8 were adopted to analyze the redesigned 48-bus DSN resilience simulation results since there is no universally accepted standard power system resilience metric at the time of compilation of this study report [22], [57].

V. PRE-HURRICANE DSN SIMULATION RESULTS ANALYSIS

A. EVALUATION OF THE EFFECTIVENESS OF THE PROPOSED BN-DSN PREDICTIVE MODEL AND HYBRID DSN'S LINE FC-MCS-SCENRED MODEL

To investigate the impact of the proposed system network line fault predictive algorithms as regards the DSN's operational resilience enhancement against hurricane events, three simulation case studies were considered. The simulation results are discussed in the context of the DSN's operational resilience improvement against predicted oncoming hurricane events. The simulated case scenarios include:

1) A simulation scenario where no proactive DSN reconfiguration and resource planning operation is performed against the forecasted oncoming hurricane event. In this case, the most probable DSN line's FC-MCS-SCENRED line fault scenario of Table 6 was taken to be the actual system network line fault scenario. This is because the prospective BN-DSN predictive line fault scenario in Table 3 matched this DSN line fault scenario 7, of Table 6, that recorded the maximum probability of DSN line fault due to the approaching hurricane event. Therefore, the system line fault scenario is used to simulate the active power flow on the grid to determine the expected active load loss that would be experienced. The simulated expected active load loss in this case is then used as a reference active load loss for further active load loss reduction analysis when the proactive DSN's reconfiguration and resource planning are applied using the simulated damage scenarios from the two prospective DSN predictive algorithms.
2) A simulation scenario where the pre-hurricane event system optimization is performed based on the combined statistical DSN line's FC-MCS-SCENRED prediction results of Table 6.
3) A simulation scenario where the pre-hurricane event system optimization is performed based on the BN-DSN predicted line fault scenario of Table 3.

Since the forecasted oncoming hurricane event was due to hit the 48-bus DSN in 60 minutes ahead, the DSO performs the pre-hurricane event prediction simulation to determine the DSN's most probable line fault scenarios using the two proposed predictive algorithms in this study. The analysis of the simulation results is reported in the next section.

B. ANALYSIS OF SIMULATION RESULTS OF THE PRE-HURRICANE EVENT DSN EXPECTED LOAD LOSS BASED ON THE PREDICTED MOST PROBABLE DSN LINE FAULT SCENARIO

Initially, before the hurricane event, the redesigned 48-bus DSN's peak active load demand of 3.5 p. u (35 MW) was met between the 19th and 22nd hours of the day. See Table 1. Considering Table 6, scenario 7 that matched the damage scenario in Table 3, the DSN fault scenario is regarded as the most probable DSN line fault to be experienced when the hurricane struck. In this case, the expected load shedding was simulated to be 1.365 p. u. This means 13.65 MW of loads would be unserved when the predicted oncoming hurricane event hit the DSN. Therefore, 1.365 p. u (13.65 MW) was used as the benchmark to quantify the operational resilience enhancement that would be achieved, after the application of the pre-hurricane event system optimization based on predicted DSN line fault scenarios in Tables 3 and 6 respectively.

TABLE 9. System FC-MCS-SCENRED model pre-hurricane events optimal switching sequence for the 10 scenarios (0 = open, 1 = close).

HOURS	Switching time step 5 Mins	RCS 1(8-9)	RCS 2 (9-17)	RCS 3(18-19)	RCS 4 (21-30)	RCS 5 (30-31)	RCS 6 (31-48)	RCS 7 (38-39)	RCS 8 (42-44)	RCS 9 (25-27)	Total switching time (Mins)
12:00 Noon	Initial RCS Status	1	0	1	0	1	0	1	1	1	Initial switching status
12:00 AM -13:00 PM	0-1	1	1	0	1	1	0	1	1	0	20 min.
13:00PM –12:00 AM	1-24	1	1	1	1	1	0	1	1	1	5 min.

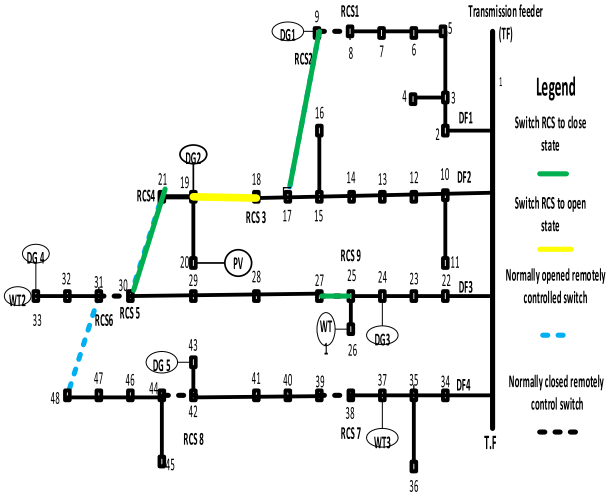

FIGURE 10. Pre-hurricane event optimal network reconfiguration and resource planning (0-1 hour).

TABLE 10. Pre-hurricane events optimal DGs planning (scheduled = 1, otherwise = 0) between 0-1 hour).

DGs location	13:00	13:05	13:10	13:15	13:20	13:25	13:30	13:35	13:40	13:45	13:50	13:55	14:00
9	1	1	1	1	1	1	1	1	1	1	1	1	1
19	0	0	0	0	1	1	1	1	1	1	1	1	1
24	1	0	1	0	0	0	0	0	0	0	0	0	0
33	0	0	0	0	1	1	1	1	1	1	1	1	1
43	1	1	1	1	1	1	1	1	1	1	1	1	1

Decrease in expected active load unserved of 13.65 MW using the DSN line fault prediction scenarios from both BN-DSN and combined statistical DSN's line FC-MCS-SCENRED predictive algorithms are of the main interest in this comparative analysis study.

C. THE DSN LINE'S FC-MCS-SCENRED BASED PRE-HURRICANE-EVENTS SYSTEM OPTIMIZATION SIMULATION RESULTS ANALYSIS

The objective function is to minimize the expected load loss via pre-hurricane events' optimal DSN reconfiguration and resource planning, via optimal switching sequence of the RCS operations. The pre-hurricane event system optimization simulation solution was proven optimal with a CPLEX execution time of 1.78 seconds. The MILP optimization solution of 2.263 p. u (22.63 MW) with its absolute and relative optimality gap of zero (0), was obtained. Optimal load shedding of 1.237 p. u (12.37 MW) was recorded over all the possible reduced predicted 10 system line fault scenarios in Table 6. The MILP program generates one optimal DSN reconfiguration switching sequence and resource planning shown in Table 9 and Fig. 10, respectively. These actions are capable of minimizing the expected load shedding over all the reduced predicted 10 DSN line fault scenarios in Table 6. Table 9 shows the pre-hurricane optimal switching sequence to mitigate the impact of the forecasted oncoming hurricane event on the DSN. Initially, the RCS 1, 3, 5, 7, 8, and 9 are normally closed switches whereas the RCS 2, 4, and 6 are normally open switches. The simulated optimal switching sequence for the first 60 minutes shows that RCS 2 was closed from the initial open state, RCS 3 was opened from the initial closed state, RCS 4 was closed from the initial open state, and RCS 9 was opened from the initial close state position. The total pre-event switching time of 20 minutes was recorded. After 1 hour, switch RCS 3 and 9 were now closed. The simulated optimal pre-hurricane event DSN's DGs planning is presented in Table 10. The corresponding hourly (0-1 hour) DG's active and reactive power planning are presented in Table 11. In Table 12, the active and reactive power output of the scheduled PV and WTs against the oncoming hurricane event is presented. Fig. 11 shows that the voltage magnitudes of all the buses in the redesigned 48-bus DSN are within the DSN normal operating condition voltage magnitudes of $0.95 \leq |V| \leq 1.05$ respectively when power flow analysis was performed indicating the steady state performance of the system network operating condition.

TABLE 11. An hour (0-1) before the hurricane event, DG scheduling.

Hour (H)	Nodes	Active power hourly DGs output (p.u)	Reactive power hourly DGs output (p.u)
13:00	9	0.020	0.055
	24	0.050	0.040
	43	0.500	0.400
13:05	9	0.020	0.210
	43	0.500	0.400
13:10	9	0.089	-0.400
	24	0.050	0.040
	43	0.500	0.400
13:15	9	0.500	0.400
	43	0.500	0.400
13:20	9	0.020	-0.400
	19	0.050	0.040
	33	0.050	0.040
	43	0.500	0.400
13:25	9	0.020	-0.400
	19	0.050	0.040
	33	0.050	0.040
	43	0.500	0.400
13:30	9	0.020	0.400
	19	0.050	0.040
	33	0.050	0.040
	43	0.500	0.400
13:35	9	0.500	-0.400
	19	0.050	0.040
	33	0.050	0.040
	43	0.500	0.400
13:40	9	0.500	-0.400
	19	0.050	0.040
	33	0.050	0.040
	43	0.500	0.400
13:45	9	0.020	0.400
	19	0.050	0.040
	33	0.050	0.040
	43	0.500	0.400
13:50	9	0.500	0.400
	19	0.050	0.040
	33	0.050	0.040
	43	0.500	0.400
13:55	9	0.020	-0.400
	19	0.050	0.040
	33	0.050	0.040
	43	0.500	0.400
14:00	9	0.500	-0.400
	19	0.050	0.040
	33	0.050	0.040
	43	0.500	0.400

D. PRE-HURRICANE EVENT SYSTEM OPTIMIZATION SIMULATION RESULTS ANALYSIS BASED ON THE PROSPECTIVE BN-DSN PREDICTIVE MODEL

In this section, the objective function of the pre-hurricane event system optimization is to minimize the expected load loss on the redesigned 48-bus DSN using the prospective BN-DSN line fault prediction scenario. The simulated solution was proven optimal with a CPLEX execution time of 1.56 seconds. The variable objective function of the MILP solution of 2.425 p. u (24.25 MW) with relative and absolute optimality gap of 0.085819 and 1.5228 respectively were obtained. Table 13 provides information about the pre-hurricane event DSN optimal switching actions for this case. The total switching time recorded was 20 minutes. with the assumed 5 minutes. each, switching time-step. The graphical representation of the switching sequence leading to proactive optimal network reconfiguration and resource scheduling based on the BN-DSN predictive line faults of Table 3 is presented in Fig. 12. Information concerning hourly scheduling of the DSN's DG can be found in Table 14. The hourly DER active power planning is

TABLE 12. An hour (0-1 hour) before hurricane event PV and WTs' active power output scheduling.

Time-step	Nodes	PV		WT 1		WT2		WT3	
Time-step	Nodes 20,26 33,37	Active power (p. u)	Reactive power (p. u)	Active power (p. u)	Reactive power (p. u)	Active power (p. u)	Reactive power (p. u)	Active power (p. u)	Reactive power (p. u)
13: 00	20,26 33,37	0.0 14	0.0 37	0.0 75	0.0 37	0.5 75	0.2 87	0.0 50	0.0 25
13: 05	20,26 33,37	0.0 75	0.0 37	0.0 75	0.0 37	0.5 75	0.2 87	0.0 50	0.0 25
13: 10	20,26 33,37	0.0 75	0.0 37	0.0 75	0.0 37	0.5 75	0.2 87	0.0 50	0.0 25
13: 15	20,26 33,37	0.0 75	0.0 37	0.0 75	0.0 37	0.5 75	0.1 04	0.0 50	0.0 25
13: 20	20,26, 33,37	0.0 75	0.0 37	0.0 75	0.0 37	0.5 75	0.2 87	0.0 50	0.0 25
13: 25	20,26 33,37	0.0 75	0.0 37	0.0 75	0.0 37	0.5 75	0.2 87	0.0 50	0.0 25
13: 30	20,26 33,37	0.0 75	0.0 37	0.0 75	0.0 37	0.5 75	0.2 87	0.0 50	0.0 25
13: 35	20,26, 33,37	0.0 75	0.0 37	0.0 75	0.0 37	0.5 75	0.2 87	0.0 50	0.0 25
13: 40	20,26, 33,37	0.0 75	0.0 37	0.0 75	0.0 37	0.5 75	0.2 87	0.0 50	0.0 25
13: 45	20,26, 33,37	0.0 75	0.0 37	0.0 75	0.0 37	0.5 75	0.2 87	0.0 50	0.0 25
13: 50	20,26, 33,37	0.0 75	0.0 37	0.0 75	0.0 37	0.5 75	0.2 87	0.0 50	0.0 25
13: 55	20,26, 33,37	0.0 75	0.0 37	0.0 75	0.0 37	0.5 75	0.2 87	0.0 50	0.0 25
14: 00	20,26,3 3,37	0.0 75	0.0 37	0.0 75	0.0 37	0.5 75	0.2 87	0.0 50	0.0 25

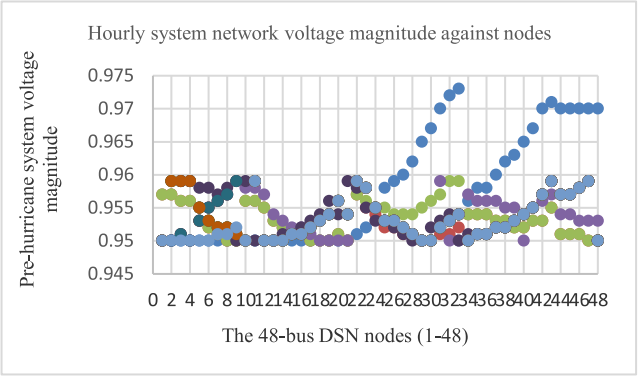

FIGURE 11. The pre-hurricane event DSN voltage magnitude monitoring report at all 48- bus DSN nodes.

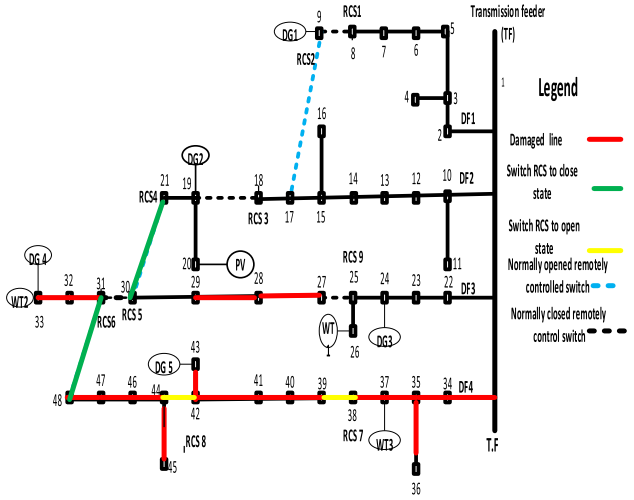

FIGURE 12. The pre-hurricane event DSN reconfiguration and resource planning based on Table 3.

TABLE 13. BN-DSN based pre-Hurricane events optimal switching sequence for the scenario 7 (0 = open, 1 = close).

Switching Time step 5 minutes	RCS1(8-9)	RCS2(9-17)	RCS3(18-19)	RCS4(21-30)	RCS5(30-31)	RCS6(31-48)	RCS7(38-39)	RCS8(42-44)	RCS9(25-27)	Total switching time (Minutes)
OPTIMAL HOURLY DSN SWITCHING SEQUENCE										
Initial RSC status	1	0	1	0	1	0	1	1	1	Initial switching status
0-24	1	0	1	1	1	1	0	0	1	20min.

TABLE 14. Pre-hurricane event status of DGs, scheduled (1) otherwise (0).

Nodes	0 (H)	1-24 (H)
9	1	1
19	0	1
24	0	1
33	1	1
43	1	1

presented in Table 15. All the BN-DSN based pre-event voltage magnitudes of all buses are within the allowable voltage range of $0.95 \leq |V| \leq 1.05$ respectively. The analysis of the system optimization simulation results in this paper for the three cases study showed decrease in the initial expected load loss from 39% to 35.34%, and finally to 30.71% respectively (See Table 16). The pre-hurricane event simulation time of 1.78 seconds and 1.56 seconds were recorded for each system optimization simulation using the two predictive models. The simulation time in both cases was less than 2 minutes. confirming the efficacy of the formulated system optimization problems in Section IV-A. The reduction in the expected load loss simulated, simply means a reduction in the expected loss of revenue to the power utility company.

TABLE 15. Pre-hurricane event hourly DER's active power output scheduling.

Hours (H)/Nodes	DERs (p.u)					PV (p.u)	WT1 (p.u)	WT2 (p.u)	WT3 (p.u)
Nodes	9	19	24	33	43	20	26	33	37
0	0.500	-	-	0.008	0.048	0.002	0.075	0.064	0.040
1-7	0.212	0.050	0.050	0.008	0.048	0.002	0.075	0.064	0.040
8	0.212	0.050	0.050	0.008	0.048	0.060	0.075	0.064	0.040
9	0.221	0.050	0.050	0.008	0.049	0.062	0.075	0.067	0.041
10	0.221	0.050	0.050	0.008	0.049	0.075	0.075	0.067	0.041
11	0.221	0.050	0.050	0.008	0.049	0.075	0.075	0.067	0.041
12	0.221	0.050	0.050	0.008	0.049	0.075	0.075	0.067	0.041
13	0.221	0.050	0.050	0.008	0.049	0.075	0.075	0.067	0.041
14	0.221	0.050	0.050	0.008	0.049	0.075	0.075	0.067	0.041
15	0.221	0.050	0.050	0.008	0.049	0.075	0.075	0.067	0.041
16	0.221	0.050	0.050	0.008	0.049	0.075	0.075	0.067	0.041
17	0.221	0.050	0.050	0.008	0.049	0.050	0.075	0.067	0.041
18	0.221	0.050	0.050	0.008	0.049	0.050	0.075	0.067	0.041
19	0.221	0.050	0.050	0.008	0.049	0.020	0.075	0.067	0.041
20-24	0.221	0.050	0.050	0.008	0.049	0.002	0.075	0.067	0.041

TABLE 16. One hour redesigned 48-bus DSN optimization simulation results for Tables 3 and 6.

Case studies with:	Daily total active energy supplied on the DSN (MWh)	% of Energy expected, not served	% of Energy supplied considering the predicted damage scenarios
No pre-hurricane event system optimization	35.00	39.00	61.00
Pre-event system optimization based on system FC-MCS-SCENRED model	35.00	35.34	64.66
Pre-event system optimization based on BN-DSN model	35.00	30.71	69.29

This justifies the fact that the proposed proactive predictive BN-DSN line fault model that produced the least expected load loss improves system operational resilience against hurricane events, when compared to the proposed combined statistical DSN line's FC-MCS-SCENRED predictive model. The impact of the prospective predictive BN-DSN line fault

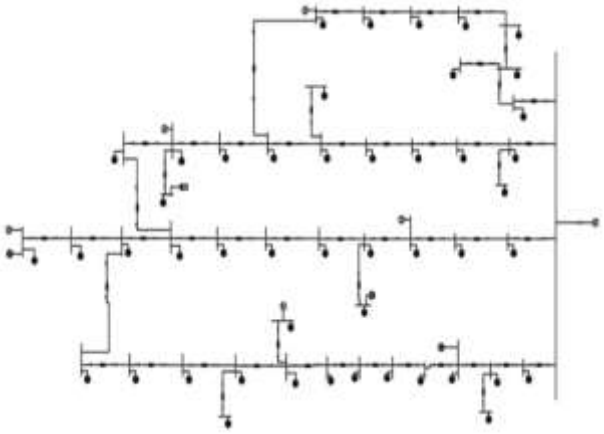

FIGURE 13. Modelling of the redesigned 48-bus BN-DSN line fault scenario using ETAP.

model as it enhances the DSN resilience proactively against hurricane events from an operational point of view has been demonstrated.

E. SYSTEM OPTIMIZATION SIMULATION RESULTS VALIDATION WITH ETAP

To validate the system optimization simulation results of the prospective BN-DSN model, the redesigned 48-bus DSN line fault in Table 3 was used to model a fault scenario on Electrical Transient Analyzer Program (ETAP) platform. However, ETAP was unable to handle a stochastic system optimization which is possible with Table 6. Fig. 13 shows the modelled redesigned 48-bus DSN network in ETAP. The load restoration data of 2.441 p. u (24.41 MW) reported in Table 17 is similar to the restoration values of 2.425 p. u (24.25 MW) obtained for the pre- hurricane event system optimization simulation result based on the prospective predictive BN-DSN model in Section V(D). Thereby validating the accuracy of the proposed system restoration scheme employed for the system optimal pre-hurricane event network reconfiguration and resource planning in this study.

VI. CONCLUSION

In this article, the pre-hurricane event DSN optimization simulation results have been analyzed to showcase the impact of the two proposed resilience evaluation methods as regards to proactively enhancing the operational resilience planning of the DSN against the predicted oncoming hurricane event.

Firstly, the efficiency of the proposed BN-DSN predictive model was compared with that of the hybrid statistical DSN line's FC-MCS-SCENRED predictive model. It was demonstrated that the stochastic pre-hurricane event system optimization simulation performed using 10 reduced DSN line fault scenarios attained optimality at a CPLEX optimizer time of 1.78 seconds whereas the pre-hurricane event system optimization simulation that was based on the prospective

TABLE 17. ETAP power flow analysis to validate the prospective BN-DSN pre-event system optimization result of GAMS.

Stages of event	Total generated load		Total supplied load		Total load demand		Total line loss		Total load shedding	
	Active (MW)	Reactive (MVar)	Active (MW)	Reactive (MVar)	Active (MW)	Reactive (MVar)	Active (MW)	Reactive (MVar)	Active (MW)	Reactive (Mvar)
Normal load flow	35.94	12.47	35.00	12.13	35.00	12.47	0.94	0.340	-	-
Pre-event DSN-load-flow	21.60	7.43	21.35	7.34	21.35	7.43	0.25	0.09	13.65	4.69
Total active and reactive load restoration via optimal network reconfiguration										
Load restore	24.80	8.66	**24.41**	8.66	25.18	8.80	0.38	0.14	10.20	3.47

BN-DSN line fault scenario converged at a CPLEX optimizer time of 1.56 seconds. From these simulation results, it can be deduced that if the predictive hybrid statistical DSN line's FC-MCS-SCENRED model's 1000-line fault scenarios were not optimally reduced to 10, using the DSN line FC-MCS-SCENRED model, the 1000 DSN line fault scenarios would have resulted in higher computational time during stochastic system optimization, compared to the system optimization simulation time of 1.56 seconds that was seen in the case of system optimization simulation based on the prospective BN-DSN line fault scenario. Inferentially, the prospective proposed BN-DSN predictive model can significantly enhance the pre-hurricane event DSN operational planning at a reduced system optimization simulation time compared to the combined statistical DSN line's FC-MCS-SCENRED predictive algorithm. The reduction in simulation time will lead to improved electricity end-users' survivability before and after hurricane events, and also reduce the revenue deficit to the power utility companies in future. However, it is very important to note that to implement the state-of-the-art algorithms' solvers for the prospective BN-DSN structure learning problem, an adaptive search technique, precisely the Branch and Bound method, and integer linear programming technique are required. Currently, we noticed that there is no single solver that dominates the other in speed. Therefore, the number of DSN line fault scenarios to be optimized would always determine the system

computational time in any case scenario as shown in this study.

Secondly, to assess the DSN operational resilience enhancement level against hurricane events, the predicted most probable DSN line fault scenario was used to perform load flow analysis. 1.365 p. u (13.65 MW) load loss was recorded without any pre-event system optimization scheme. With system optimization based on the prospective hybrid statistical DSN line's FC-MCS-SCENRED predicted DSN line damage scenario 1.365 p. u (13.65 MW) active power supply loss was reduced to 1.237 p. u (12.37 MW) at 1.78 seconds simulation time, with 25 minutes switching time respectively. Similarly, the pre-event system optimization that was carried out based on the prospective BN-DSN predictive model, also reduced the expected load loss from 1.365 p. u (13.65 MW) to 1.075 p. u (10.75 MW) at 1.56 seconds with 20 minutes switching time. The ETAP simulator system optimization results confirmed the correctness of the system optimization results from the BN-DSN system optimization. Therefore, with the reduction in active load shedding, and switching time, it is reasonable to conclude that the predictive BN-DSN line fault model helps the DSO to operationally plan and prepare the redesigned 48-bus DSN against the forecasted oncoming hurricane event, to lessen the hurricane event's impact on the DSN significantly.

Conclusively, the comparative analysis study on the DSN operational resilience enhancement model against HILL events in this article showcases the usefulness of the predictive algorithms as system resilience evaluation techniques. It is demonstrated that the pre-hurricane events system optimization built on the predictive BN-DSN line fault model can greatly enhance the operational resilience of the DSN against hurricane events in the future to reduce the expected active power supply loss when compared with the load loss reduction obtained using hybrid statistical DSN line's FC-MCS-SCENRED predictive model. However, the goal of the DSO is to minimize the load shedding and restore the DSN to normal operational status in the shortest possible time in any case of contingency. In this study, total restoration of the DSN loads is not possible under this research scope. This article did not cover the system components' hardening that bothered on infrastructural resilience improvement planning. In such a situation, one of the reported problems of the infrastructural resilience improvement is insufficient funding or the high cost of system hardening. Therefore, to achieve total power supply restoration in future research, a cost-effective hardening and operational system resilience improvement algorithm is recommended to be developed as a combinatorial optimization approach to solve the probabilistic load restoration problem under both the operational and infrastructural planning approaches. In the same vein, the use of renewable energy resources to serve the loads after a hurricane event is promising in enhancing the system performance. However, the uncertainty associated with DER energy productions because they are weather dependent is a major problem that needs holistic research investigation for proper proactive planning to meet the load demand after hurricane events. It is therefore recommended that this model be developed to improve this current research results in the future.

ACKNOWLEDGMENT

Authors ackowledge the contributions of Boda Li et al., [19] for providing the hurricane historical data utilized in this research. Appreciation goes to Babak Taheri et al., [18], [48], for their contributions during the formulation of the system optimization problems and simulation codes utilized in this study.

CONFLICT OF INTEREST

Authors declare that there is no conflict of interest in this research.

REFERENCES

[1] P. Hines, J. Apt, and S. Talukdar, "Trends in the history of large blackouts in the United States," *Proc. IEEE Power Energy Soc. Gen. Meeting*, vol. 37, no. 1, pp. 5249–5259, Jul., 2009, doi: 10.1109/PES.2008.4596715.

[2] P. Hines, J. Apt, and S. Talukdar, "Large blackouts in North America: Historical trends and policy implications," *Energy Policy*, vol. 37, no. 12, pp. 5249–5259, Dec. 2009, doi: 10.1016/j.enpol.2009.07.049.

[3] R. J. Campbell. (2012). *Weather-Related Power Outages and Electric System Resiliency*. Accessed: Oct. 2, 2020. [Online]. Available: https://www.crs.gov

[4] GFDL. *Global Warming and Hurricanes—Geophysical Fluid Dynamics Laboratory*. Accessed: Oct. 2, 2020. [Online]. Available: https://www.gfdl.noaa.gov/global-warming-and-hurricanes

[5] *Tropical Storm Ewiniar*, Wikipedia, Vietnam, Jun. 2018. Accessed: Oct. 2, 2020. [Online]. Available: https://en.wikipedia.org/wiki/tropical_storm_Ewiniar_(2018)

[6] *Tropical Storm Ewiniar Landfall in China Seen by NASA's Aqua Satellite*, Goddard Space Flight Center, Greenbelt, MD, USA, 2018.

[7] Wikipedia. (2021). *Tropical Cyclones in Southern Africa*. Accessed: Oct. 2, 2020. [Online]. Available: https://en.wikipedia.org/wiki/Tropical_cyclones_in_Southern_Africa

[8] J. V. Tom Batchelor, A. Jamieson, A. Gregory, and G. Kilander. (2021). *Second Person Dies as a Million in Louisiana and Mississippi Face Weeks Without Power in Aftermath of 'Catastrophic' Hurricane—Follow Live Updates_The Independent TV*. United States America. [Online]. Available: https://centralmnbuzz.com/author/e8ec1c1a2ad85b0ba32f178c0ee059fe

[9] *Power Outages Have Spiked in the Past 10 Years*, RC Ramirez, CNN, Atlanta, GA, USA, 2022.

[10] *Lagos Flood: EKEDC Restores Electricity to Lekki, Ikoyi, Victoria Island*, P-Times, Lagos, pp. 1–6, Oct. 2022.

[11] A Report, "Nigeria's floodwaters reveal a state unable to protect its people," France, Afr. Rep., 2022, pp. 1–5. [Online]. Available: https://www.theafricareport.com/254513/nigerias-floodwaters-reveal-a-state-unable-to-protect-its-people/

[12] O. S. Omogoye, K. A. Folly, and K. O. Awodele, "Review of sequential steps to realize power system resilience," in *Proc. Int. SAUPEC/RobMech/PRASA Conf.*, Cape Town, South Africa, Jan. 2020, pp. 1–6, doi: 10.1109/SAUPEC/RobMech/PRASA48453.2020.9040967.

[13] A. M. Stankovic, "Methods for analysis and quantification of power system resilience," *IEEE Trans. Power Syst.*, vol. 14, no. 8, pp. 1–14, Oct. 2022, doi: 10.1109/tpwrs.2022.3212688.

[14] Z. Bie, Y. Lin, G. Li, and F. Li, "Battling the extreme: A study on the power system resilience," *Proc. IEEE*, vol. 105, no. 7, pp. 1253–1266, Jul. 2017, doi: 10.1109/JPROC.2017.2679040.

[15] O. S. Omogoye, K. A. Folly, and K. O. Awodele, "Review of proactive operational measures for the distribution power system resilience enhancement against hurricane events," in *Proc. Southern Afr. Universities Power Eng. Conference/Robotics Mechatronics/Pattern Recognit. Assoc. South Afr. (SAUPEC/RobMech/PRASA)*, Potchefstroom, South Africa, Jan. 2021, pp. 1–6, doi: 10.1109/SAUPEC/RobMech/PRASA52254.2021.9377252.

[16] O. S. Omogoye, K. A. Folly, and K. O. Awodele, "A review of power system predictive failure model for resilience enhancement against hurricane events," *J. Eng.*, vol. 2021, no. 11, pp. 644–652, Oct. 2021, doi: 10.1049/tje2.12092.

[17] Y. Lin, Z. Bie, and A. Qiu, "A review of key strategies in realizing power system resilience," *Global Energy Interconnection*, vol. 1, no. 1, pp. 70–78, Jan. 2018, doi: 10.14171/j.2096-5117.gei.2018.01.009.

[18] B. Taheri, A. Safdarian, M. Moeini-aghtaie, and M. Lehtonen, "Enhancing resilience level of power distribution systems using proactive operational actions," *IEEE Access*, vol. 7, pp. 1–13, 2019, doi: 10.1109/ACCESS.2019.2941593.

[19] B. Li, Y. Chen, S. Huang, H. Guan, Y. Xiong, and S. Mei, "A Bayesian network model for predicting outages of distribution system caused by hurricanes," in *Proc. IEEE Power Energy Soc. General Meeting (PESGM)*, Montreal, QC, Canada, Aug. 2020, pp. 1–6, doi: 10.1109/PESGM41954.2020.9281923.

[20] O. S. Omogoye, K. A. Folly, and K. O. Awodele, "Distribution system network resilience enhancement against predicted hurricane events using statistical probabilistic system line damage prediction model," in *Proc. IEEE PES/IAS PowerAfrica*, Nairobi, Kenya, Aug. 2021, pp. 1–5, doi: 10.1109/powerafrica52236.2021.9543464.

[21] O. S. Omogoye, K. A. Folly, and K. O. Awodele, "Enhancing the distribution power system resilience against hurricane events using a Bayesian network line outage prediction model," *J. Eng.*, vol. 2021, no. 11, pp. 731–744, Oct. 2021, doi: 10.1049/tje2.12091.

[22] N. Bhusal, M. Abdelmalak, M. Kamruzzaman, and M. Benidris, "Power system resilience: Current practices, challenges, and future directions," *IEEE Access*, vol. 8, pp. 18064–18086, 2020, doi: 10.1109/ACCESS.2020.2968586.

[23] (2017).*3 Storms, 3 Responses_Comparing Harvey, Irma and Maria—CNN*. USA. [Online]. Available: https://www.cnn.com/2017/09/27

[24] M. Rahmani-Andebili and M. Fotuhi-Firuzabad, "An adaptive approach for PEVs charging management and reconfiguration of electrical distribution system penetrated by renewables," *IEEE Trans. Ind. Informat.*, vol. 14, no. 5, pp. 2001–2010, May 2018, doi: 10.1109/TII.2017.2761336.

[25] S. O. Omogoye, K. A. Folly, and K. O. Awodele, "Situation awareness to enhance the distribution system network operational resilience against hurricane event," in *Proc. IEEE PES/IAS PowerAfrica*, Kigali, Rwanda, Aug. 2022, pp. 1–5, doi: 10.1109/PowerAfrica53997.2022.9905356.

[26] S. R. Han, "Estimating hurricane outage and damage risk in power distribution systems," Ph.D. dissertation, Dept. Civil Eng., Texas A&M Univ., College Station, TX, USA, 2008.

[27] R. W. Wolfe and R. O. Kluge, "Designated fiber stress for wood poles," Forest Products Laboratories, Madison, WI, USA, 2002, pp. 1–42.

[28] M. M. Alam, B. Eren Tokgoz, and S. Hwang, "Framework for measuring the resilience of utility poles of an electric power distribution network," *Int. J. Disaster Risk Sci.*, vol. 10, no. 2, pp. 270–281, May 2019, doi: 10.1007/s13753-019-0219-8.

[29] F. Taroni, A. Biedermann, S. Bozza, P. Garbolino, and C. Aitken, *Bayesian Networks for Probabilistic Inference and Decision Analysis in Forensic Science* 2nd ed. Chichester, U.K.: Wile, 2014, pp. 1–473. [Online]. Available: http://www.pdf.net

[30] J. Pearl, *Probabilistic Reasoning in Intelligent Systems: Networks of Plausible Inference*, 2nd ed. San Francisco, CA, USA: Morgan Kaufmann, 1990, pp. 1–573, doi: 10.1017/CBO9781107415324.004.

[31] K. Murphy, "A variational approximation for Bayesian networks with discrete and continuous latent variables," 2013, *arXiv:1301.6724*.

[32] I. H. Kong, T. Po, and I. H. Kong, "Tropical storm Ewiniar," Wikipedia, Tech. Rep., 2018. [Online]. Available: https://en.wikipedia.org/w/index.php?title=Tropical_Storm_Ewiniar_(2018)&Oldid=1014097293

[33] K. Murphy. *BNT-Master*. Accessed: Oct. 2, 2020. [Online]. Available: https://github.com/bayesnet/bnt

[34] D. Oehm. (2019). Simulating Data With Bayesian Networks. WordPress. Accessed: Nov. 10, 2020. [Online]. Available: https://gradientdescending.com

[35] G. A. Pagani and M. Aiello, "The power grid as a complex network: A survey," *Phys. A, Statist. Mech. Appl.*, vol. 392, no. 11, pp. 2688–2700, 2013, doi: 10.1016/j.physa.2013.01.023.

[36] M. Sadeghi Khomami and M. S. Sepasian, "Pre-hurricane optimal placement model of repair teams to improve distribution network resilience," *Electric Power Syst. Res.*, vol. 165, pp. 1–8, Dec. 2018, doi: 10.1016/j.epsr.2018.08.016.

[37] R. N. Allan and R. Billinton, "Basic probability and reliability concepts," in *Reliability Evaluation of Power Systems*. New York, NY, USA: Springer, 1996, pp. 1–136. [Online]. Available: https://link.springer.com, doi: 10.1007/978-1-4615-7731-7.

[38] M. Panteli, P. Mancarella, D. N. Trakas, E. Kyriakides, and N. D. Hatziargyriou, "Metrics and quantification of operational and infrastructure resilience in power systems," *IEEE Trans. Power Syst.*, vol. 32, no. 6, pp. 4732–4742, Nov. 2017, doi: 10.1109/TPWRS.2017.2664141.

[39] S. Poudel, A. Dubey, and A. Bose, "Risk-based probabilistic quantification of power distribution system operational resilience," *IEEE Syst. J.*, vol. 14, no. 3, pp. 1–12, Sep. 2020, doi: 10.1109/JSYST.2019.2940939.

[40] R. Billinton and W. Li, *Reliability Assessment of Electric Power Systems Using Monte Carlo Methods*. New York, NY, USA: Springer, 2013, doi: 10.1007/978-1-4899-1346-3.

[41] N. Gröwe-Kuska, "Gams/scenred," Inst. Math. (Vattenfall Europe Trading Gmbh), Humboldt Univ., Berlin, Germany, Tech. Rep., 2003, pp. 1–12.

[42] J. M. Wilson, "Introduction to stochastic programming," *J. Oper. Res. Soc.*, vol. 49, no. 8, pp. 897–898, 1998, doi: 10.1057/palgrave.jors.2600031.

[43] P. Thoft-Chistensen and Y. Murotsu, "The branch-and-bound method," in *Application of Structural Systems Reliability Theory*. Berlin, Germany: Springer, 1986, doi: 10.1007/978-3-642-82764-8_7.

[44] *Release Notes–GAMS/SCENRED Introduced*, M Ready, GAMS Distrib., 2002, pp. 713–719. [Online]. Available: https://gamsworld.gams.com

[45] J. Zhu, *Optimization of Power System Operation*, 2nd ed. Hoboken, NJ, USA: Wiley, 2009, pp. 1–623. [Online]. Available: http://www.pdf.net

[46] A. L. Morelato and A. Monticelli, "Heuristic search approach to distribution system restoration," *IEEE Trans. Power Del.*, vol. 4, no. 4, pp. 2235–2241, Oct. 1989, doi: 10.1109/61.35652.

[47] E. R. Ramos, A. G. Exposito, J. R. Santos, and F. L. Iborra, "Path-based distribution network modeling: Application to reconfiguration for loss reduction," *IEEE Trans. Power Syst.*, vol. 20, no. 2, pp. 556–564, May 2005, doi: 10.1109/TPWRS.2005.846212.

[48] B. Taheri, A. Safdarian, M. Moeini-Aghtaie, and M. Lehtonen, "Distribution systems resilience enhancement via pre- and post-event actions," *IET Smart Grid*, vol. 2, no. 4, pp. 549–556, Jul. 2019, doi: 10.1049/iet-stg.2019.0035.

[49] B. Taheri, A. Jalilian, A. Safdarian, M. Moeini-Aghtaie, and M. Lehtonen, "Toward operational resilience of smart energy networks in complex infrastructures," in *Optimization, Learning, and Control for Interdependent Complex Networks. Advances in Intelligent Systems and Computing*, M. Amini, Eds. vol. 1123. Cham, Switzerland: Springer, 2020, doi: 10.1007/978-3-030-34094-0_9.

[50] M. S. Khomami, K. Jalilpoor, M. T. Kenari, and M. S. Sepasian, "Bi-level network reconfiguration model to improve the resilience of distribution systems against extreme weather events," *IET Gener., Transmiss. Distrib.*, vol. 13, no. 15, pp. 3302–3310, May 2019, doi: 10.1049/iet-gtd.2018.6971.

[51] M. E. Baran and F. F. Wu, "Optimal capacitor placement on radial distribution systems," *IEEE Trans. Power Del.*, vol. 4, no. 1, pp. 725–734, Jan. 1989, doi: 10.1109/61.19265.

[52] Wikipedia. (2011). *Big M Method: Linear Programming*. Accessed: May 10, 2021. [Online]. Available: http://www.universalteacherpublications.com/univ/ebooks/or/Ch3/mmethod.htm

[53] M. H. Amirioun, F. Aminifar, and H. Lesani, "Resilience-oriented proactive management of microgrids against windstorms," *IEEE Trans. Power Syst.*, vol. 33, no. 4, pp. 4275–4284, Jul. 2018, doi: 10.1109/TPWRS.2017.2765600.

[54] M. R. Sarker, M. A. Ortega-Vazquez, and D. S. Kirschen, "Optimal coordination and scheduling of demand response via monetary incentives," *IEEE Trans. Smart Grid*, vol. 6, no. 3, pp. 1341–1352, May 2015, doi: 10.1109/TSG.2014.2375067.

[55] R. A. Jabr, R. Singh, and B. C. Pal, "Minimum loss network reconfiguration using mixed-integer convex programming," *IEEE Trans. Power Syst.*, vol. 27, no. 2, pp. 1106–1115, May 2012, doi: 10.1109/TPWRS.2011.2180406.

[56] B. A. McCarl, "McCarl GAMS user guide, version 22.6," GAMS Cooperation, Texax A&M Univ., College Station, TX, USA, Tech. Rep., 2008. [Online]. Available: https://www.gams.com/mccarlGulde

[57] I. Hadachi and S. Albayrak, "A survey on simulation of power systems resilience under extreme weather events," in *Proc. IEEE Milan PowerTech*, Milan, Italy, Jun. 2019, pp. 1–6, doi: 10.1109/PTC.2019.8810541.

SAMUEL O. OMOGOYE (Member, IEEE) was born in Ilorin, Kwara State, Nigeria. He received a B.Tech. degree in Electronic and Electrical Engineering from Ladoke Akintola University of Technology (LAUTECH), Ogbomoso, Oyo-State, Nigeria in 2006. He obtained his M.Sc. degree in Electrical Engineering (Power systems option) from University of Lagos (UNILAG), Akoka, Lagos State, Nigeria, in 2014. He got his Ph.D. degree in Electrical Engineering from the Department of Electrical Engineering, University of Cape Town, Cape Town, South Africa, in 2022. His areas of research interests include power system resilience enhancement, power system reliability, and the application of artificial intelligence strategies to strengthen power system operational planning.

Dr. Omogoye is a registered Engineer with the Council for the Regulation of Engineering in Nigeria (COREN R20, 293) and a Graduate Member of the Nigerian Society of Engineers (GMNSE G7960). His publications can be found on https://www.researchgate.net/profile/Samuel-Omogoye

KOMLA A. FOLLY (Senior Member, IEEE) received the B.Sc. and M.Sc. degrees in Electrical Engineering from Tsinghua University, Beijing, China, in 1989 and 1993, respectively, and the Ph.D. degree in Electrical Engineering from Hiroshima University, Japan, in 1997.

From 1997 to 2000, he was with the Central Research Institute of Electric Power Industry (CRIEPI), Tokyo, Japan. In 2009, he received a Fulbright Scholarship and was a Fulbright Scholar with the Missouri University of Science and Technology, Rolla, MO, USA. He is currently a Professor with the Department of Electrical Engineering, University of Cape Town, Cape Town, South Africa. His research interests include power system stability, control and optimization, high-voltage direct current modeling, the network integration of renewable energy, the application of artificial intelligence computation to power systems, smart grids, and power system resilience.

Prof. Folly is a member of the Institute of Electrical Engineers of Japan (IEEJ) and a fellow of the South African Institute of Electrical Engineers (SAIEE).

KEHINDE O. AWODELE (Member, IEEE) received the B.Sc. degree in Electronic and Electrical Engineering from the University of Ife (now Obafemi Awolowo University), Nigeria, in 1979, and the M.Sc. degree in Electrical Power and Machines and the PGDM degree from Ahmadu Bello University (ABU), Nigeria, in 1991 and 1999, respectively. She was involved in the electricity meter and circuit breaker manufacturing industry for several years, where she served in various capacities and received series of training with the technical partners' plants in Switzerland, Germany, and Greece, before moving to academics. She was a Lecturer with the Department of Electrical Engineering, Namibia University of Science and Technology, for some years, and later with the Department of Electrical Engineering, University of Cape Town, South Africa. Her research interests include power system reliability and resilience, distributed generation and renewable energy integration, smart grids, protection, demand side management, and power quality.

Mrs. Awodele is a registered Engineer with the Council for the Regulation of Engineering in Nigeria (COREN) and a member of the Nigeria Society of Engineers (NSE).